Critical viscoelastic behavior of colloids

Jan K. G. Dhont[1] and Gerhard Nägele[2]
[1]*Van 't Hoff Laboratory for Physical and Colloid Chemistry, Debye Research Institute, Utrecht University, Padualaan 8, 3584 CH Utrecht, The Netherlands*
[2]*Fakultät für Physik, University of Konstanz, P.O. Box 5565, D-78434 Konstanz, Germany*
(Received 30 July 1998)

The linear and nonlinear frequency-dependent viscoelastic response of a suspension of spherical colloids in the vicinity of the gas-liquid critical point is analyzed in the mean-field region. Explicit expressions for the shear rate and frequency dependence of the static structure factor are derived, starting from the *N*-particle Smoluchowski equation, which is the fundamental equation of motion for the probability density function of the position coordinates of the spherical colloids. Microscopic expressions for the anomalous parts of the linear and nonlinear response functions are derived, which are then expressed as wave-vector integrals weighted with the static structure factor. These integrals are evaluated in part numerically, leading to explicit results for the viscoelastic response functions. The critical enhancement of both the linear and nonlinear viscoelastic response functions is found to be far more pronounced than for molecular systems as a result of long-ranged hydrodynamic interactions between the colloidal particles. Viscoelastic response functions are found to diverge with the same exponent as the correlation length of the quiescent, unsheared suspension. The frequency spectrum of the linear response functions is found to be extremely broad, while nonlinearity affects only the low-frequency behavior of the lowest-order response functions. The lowest-order response functions attain their linear response values at higher frequencies even far into the nonlinear regime. Nonlinear effects are thus absent at higher frequencies. For these higher frequencies the lowest-order response functions are found to vary with the frequency ω as $\omega^{-1/4}$ close to the critical point and cross over to a $\omega^{-1/2}$ dependence further away from the critical point. In addition to the viscoelastic response of an otherwise quiescent suspension, the viscoelastic response of a stationary sheared suspension is discussed. The response of such a stationary sheared system to a superimposed oscillatory shear flow probes the dynamics of the partially distorted microstructure by the stationary shear flow. The frequency spectrum of the linear viscoelastic response functions is found to be strongly affected by the microstructure distortion due to the stationary shear flow. [S1063-651X(98)15512-5]

PACS number(s): 82.70.Dd, 05.70.Jk, 51.20.+d, 64.60.Ht

I. INTRODUCTION

The critical exponent z_η that relates the zero-shear and zero-frequency shear viscosity η of *molecular systems* to the correlation length ξ of the unsheared, quiescent system as $\eta \sim \xi^{z_\eta}$ is known to be as small as 0.06 [1], in accord with mode-coupling and renormalization group calculations [2]. The experimentally measurable critical enhancement of the viscosity is therefore only about 10–20 % relative to the background viscosity. For *colloidal systems*, the mean-field critical exponent has recently been shown to be as large as $z_\eta = 1$, both theoretically [3] and experimentally [4]. The reason for this much stronger enhancement in the vicinity of the gas-liquid critical point is the interaction between colloidal particles that is mediated via the solvent, so-called hydrodynamic interaction. This type of interaction between the colloidal particles is sufficiently long ranged to lead to a strong critical divergence of the shear viscosity. It is therefore interesting to study the full frequency dependence of the shear viscosity of colloidal systems near the critical point. Moreover, since the range of shear rates where the response is linear vanishes on approach of the critical point, due to the development of long-range correlations and slowing down of density fluctuations, it is also interesting to ask about the nonlinear response.

The role of hydrodynamic interactions between the colloidal particles is twofold. First of all, it enters the microscopic expression for the viscoelastic response functions. These microscopic expressions are ensemble averages of phase functions, among which are the hydrodynamic interaction functions. As pointed out above, these hydrodynamic interaction functions are long ranged and are responsible for the strong divergence of the viscoelastic response functions for colloids as compared to molecular systems. Second, the ensemble average that represents the viscoelastic response functions must be evaluated with respect to the shear rate distorted pair-correlation function. The shear rate dependence of this probability density function is the result of an interplay between equilibrium restoring forces and shear forces. The interplay between these forces is modified by hydrodynamic interactions, but the essential features of the shear distortion of the pair-correlation function is retaining when neglecting hydrodynamic interactions. Thus, in deriving a microscopic expression for the viscoelastic response functions one has to include hydrodynamic interactions, while for the calculation of the shear distorted pair-correlation function hydrodynamic interactions are not essential.

The viscoelastic response functions will turn out to be equal to two distinct additive contributions: an anomalous and a background contribution. The anomalous contribution is that part of the viscoelastic response function that diverges at the critical point due to the development of long-range correlations. This is the interesting part of response functions, for which predictions are made in the present paper.

 © 1998 The American Physical Society

The background contribution to the viscoelastic response functions is the viscosity that would have been measured in the absence of long-range correlations. This contribution is well behaved right up to the critical point. The background contribution must be subtracted from experimental viscoelastic response functions to obtain their anomalous contribution, which may then be compared to theoretical predictions. Nonlinear viscoelastic response functions do not have a background contribution because background contributions are in their linear response regime even when long-range correlations are affected in a nonlinear fashion.

We address linear and nonlinear response functions for a purely oscillatory shear flow and the linear reponse functions to an oscillatory shear flow orthogonally superimposed on stationary shearing motion. The results presented here allow for the analysis of a nonlinear response to oscillatory shear flow superimposed on a stationary shear flow. We restrict ourselves here to the linear response regime with respect to the superimposed oscillatory shear flow since the idea is to probe the dynamics of the stationary sheared microstructure without disrupting it too much by the oscillatory flow. Only orthogonally superimposed oscillatory shearing motion is considered, although the entire analysis is easily adapted to the case of a parallel superimposed oscillatory shear flow.

A microscopic evaluation of the viscosity consists of three steps: the calculation of the shear distorted pair-correlation function, the derivation of microscopic expressions for the viscoelastic response functions (where they are expressed in terms of an ensemble average of appropriate phase functions), and the explicit evaluation of these microscopic expressions with the use of the earlier derived pair-correlation function.

This paper is organized as follows. The flow field is defined in Sec. II. Section III contains an analysis of the structure factor under shear flow (step 1 referred to above). In Sec. III A the equation of motion for the structure factor is derived. Its solution without shear flow is shown to reproduce the well-known Ornstein-Zernike structure factor in Sec. III B. The equation of motion is written in dimensionless form in Sec. III C, and the important ''dressed'' Péclet numbers and Deborah number are introduced. The dimensionless equation of motion is solved for a stationary shear flow, in the absence of an oscillatory shear flow, in Sec. III D, while the most general equation of motion for the case of an oscillatory flow, orthogonally superimposed on a stationary shear flow, is solved in Sec. III E. The more simple case of a pure oscillatory shear flow is considered in Sec. III F. In Sec. IV the linear and nonlinear viscoelastic response functions are defined and microscopic expressions for these response functions are derived (step 2 referred to above). These microscopic expressions are evaluated in terms of the structure factor in Sec. V (step 3 referred to above), which are then expressed in terms of dimensionless scaling forms in Sec. V A. Explicit analytical and numerical results for these scaling forms of the viscoelastic response functions are presented in Secs. VI and VII. Section VI A considers pure oscillatory flow in the linear regime, Sec. VI B carries this further to the nonlinear regime, and Sec. VII is concerned with the linear response to an oscillatory shear flow, orthogonally superimposed on a stationary shear flow.

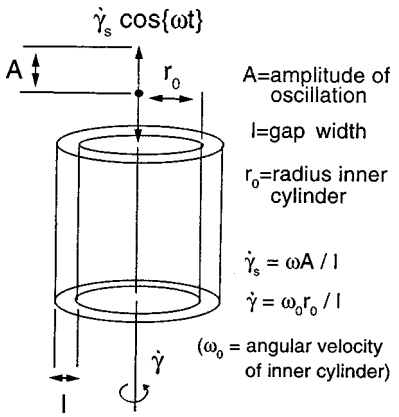

FIG. 1. Couette geometry corresponding to the velocity gradient tensor in Eq. (2).

II. FLOW FIELD

The flow field considered in the present paper is a stationary simple shear flow with an orthogonally superimposed oscillatory shear flow. The couette cell geometry corresponding to such a flow is depicted in Fig. 1. The inner (or the outer) cylinder is rotating with a constant angular frequency ω_0 and in addition exerts an oscillatory up-and-down motion with frequency ω. The fluid flow velocity $\mathbf{u}(\mathbf{r})$ at a point $\mathbf{r}$ within the gap of the couette cell is now given by

$$\mathbf{u}(\mathbf{r}) = \mathbf{\Gamma} \cdot \mathbf{r}, \tag{1}$$

where the velocity gradient matrix $\mathbf{\Gamma}$ is equal to

$$\mathbf{\Gamma} = \begin{pmatrix} 0 & \dot{\gamma} & 0 \\ 0 & 0 & 0 \\ 0 & \dot{\gamma}_s \cos\{\omega t\} & 0 \end{pmatrix}, \tag{2}$$

with $\dot{\gamma}$ and $\dot{\gamma}_s$ the shear rates corresponding to the stationary and oscillatory components of the flow, respectively. In terms of geometrical parameters of the couette cell we have $\dot{\gamma} = \omega_0 r_0 / l$ (where r_0 is the radius of the inner cylinder and l is the gap width) and $\dot{\gamma}_s = \omega A / l$ (where A is the amplitude of oscillation for the up-and-down motion of the inner cylinder).

In writing Eqs. (1) and (2) it is assumed that the velocity of the wall of the oscillating cylinder is instantaneously transferred to the entire suspension within the gap of the rheometer. Both the viscous penetration depth and the wavelength of the induced oscillatory motion of the suspension are thus assumed to be at least of the order of the gap width. The penetration depth and wavelength are both equal to $\sqrt{2\eta/\rho\omega}$, where η is the shear viscosity and ρ the mass density of the suspension [5]. For suspensions with a viscosity of a few times that of water or larger, the penetration depth and wavelength are of the order of or larger than 1 mm for frequencies $\omega < 10$ Hz. The relevant frequencies for near-critical systems are small due to critical slowing down. It should therefore be possible to perform meaningful experiments that probe the frequencies of interest as far as bulk properties are concerned. A description of the experimental

setup with which superimposed flow experiments can be performed is given in Refs. [6,7].

In a surface loading experiment, $\dot{\gamma}_s$ in Eq. (2) would be an exponentially decreasing function of the distance to the wall of the oscillating cylinder. Such high-frequency experiments are not considered here.

In the present paper we address the viscoelastic response to the oscillatory motion. Two different cases are considered: the linear and nonlinear viscoelastic response in the absence of the stationary component of the shear flow ($\dot{\gamma}=0$) and the linear viscoelastic response of a stationary sheared system. The former case is the more common situation of what is usually referred to as the dynamic viscoelastic response. In the latter case we restrict ourselves to the linear response with respect to the orthogonally superimposed oscillatory shear flow since the idea here is to probe the dynamics of a microstructure under stationary shear with a minimum perturbing effect of the oscillatory shear flow. The stationary shear rate $\dot{\gamma}$ can be large, however, such that the microstructure is nonlinearly affected by the stationary flow. The relatively most simple case of viscous response to a stationary shear flow, in the absence of the oscillatory flow, has been considered elsewhere [3] and is reproduced here as the zero-frequency limit of the pure oscillatory viscoelastic response.

III. STRUCTURE FACTOR UNDER SHEAR FLOW

In order to calculate the viscoelastic response of a suspension, an expression for the shear flow distorted pair-correlation function is needed, or, equivalently, its Fourier transform, which is essentially the structure factor. Notable theoretical approaches to describe shear flow effects on a microstructure are due to Onuki *et al.* [8,9], Schwarzl and Hess [10], Ronis [11], and Wagner and Russel [12]. The approach taken in the present section is specific for colloidal systems near their gas-liquid critical point. This appraoch leads to an equation of motion with an explicit expression for the effective diffusion coefficient and the dressed Péclet numbers and Deborah number in terms of the shear rate and the correlation length of the unsheared, quiescent dispersion.

This section is organized as follows. First of all, an equation of motion for the structure factor is derived in Sec. III A, starting from the Smoluchowski equation. Without shear flow this equation of motion is solved in Sec. III B. The solution reproduces the well-known Ornstein-Zernike expression. In Sec. III C the equation of motion is written in dimensionless form, giving rise to dressed Péclet numbers, which measure the effect of shear flow on critical density fluctuations, and a dressed Deborah number, which characterizes the frequency at which critical fluctuations cease to adapt instantaneously to the applied oscillatory shear flow. The dimensionless equation of motion is then solved in Sec. III D for the case of a stationary shear flow (where $\dot{\gamma}_s=0$) and for the general case of an orthogonally superimposed oscillatory shear flow in Sec. III E. Section III F discusses the more simple case of a pure oscillatory shear flow (where $\dot{\gamma}=0$). In all cases the expressions that are derived for the structure factor are not limited to the linear regime but extend to the nonlinear response regime.

A. Derivation of the equation of motion

The fundamental equation of motion that needs be solved is the Smoluchowski equation, which is the equation of motion for the probability density function P of the position coordinates $\{\mathbf{r}_j\}, j=1,\ldots,N$ of the N colloidal particles in the suspension [13–16],

$$\frac{\partial P}{\partial t}=D_0\sum_{j=1}^{N}\nabla_j\cdot[\nabla_j P+\beta P(\nabla_j\Phi)]-\sum_{j=1}^{N}\nabla_j\cdot[\mathbf{\Gamma}\cdot\mathbf{r}_j P], \tag{3}$$

where D_0 is the single-particle diffusion coefficient, $\beta=1/k_BT$ (with k_B Boltzmann's constant and T the temperature), ∇_j is the gradient operator with respect to $\mathbf{r}_j$, and Φ is the total potential energy of the assembly of colloidal particles. In this equation of motion we neglected hydrodynamic interactions between the colloidal particles. To describe the effect of hydrodynamic interactions on the critical behavior of P it would be sufficient to include only the long-range contributions to the hydrodynamic interaction functions. However, the essential features of the shear distorted structure are already described by Eq. (3) as the result of the interplay between equilibrium restoring direct and Brownian forces [represented by the first term on the right-hand side in Eq. (3)] and shear forces [the last term in Eq. (3)]. Hydrodynamic interactions will modify the details of the interplay between these forces but do not change the essential features of the shear induced distortion. The inclusion of hydrodynamic interactions is a future challenge.

An equation of motion for the shear-rate-dependent pair-correlation function g can be obtained from the N-particle Smoluchowski equation (3), noting that for a homogeneous system

$$g(\mathbf{r}_1,\mathbf{r}_2,t)=V^2\int d\mathbf{r}_3\cdots\int d\mathbf{r}_N P(\mathbf{r}_1,\mathbf{r}_2,\mathbf{r}_3,\cdots\mathbf{r}_N,t), \tag{4}$$

with V the volume of the system. Integration of the Smoluchowski equation (3) with respect to the coordinates $\mathbf{r}_3,\ldots\mathbf{r}_N$, assuming a pairwise additive potential energy of pair potentials V, gives (with $\mathbf{r}=\mathbf{r}_1-\mathbf{r}_2$ and ∇_r the gradient operator with respect to $\mathbf{r}$)

$$\frac{\partial g(\mathbf{r},t)}{\partial t}=2D_0\nabla_r\cdot\{\nabla_r g(\mathbf{r},t)+\beta g(\mathbf{r},t)[\nabla_r V(r)-\mathbf{F}_{\rm ind}(\mathbf{r},t)]\}$$
$$-\nabla_r\cdot[\mathbf{\Gamma}\cdot\mathbf{r}g(\mathbf{r},t)], \tag{5}$$

where (with $\mathbf{r}'=\mathbf{r}_1-\mathbf{r}_3$)

$$\mathbf{F}_{\rm ind}(\mathbf{r},t)=-\bar{\rho}\int d\mathbf{r}'[\nabla_{r'}V(r')]\frac{g_3(\mathbf{r},\mathbf{r}',t)}{g(\mathbf{r},t)}, \tag{6}$$

is the shear-rate-dependent *indirect force*. This is the force between two colloidal particles located at $\mathbf{r}_1$ and $\mathbf{r}_2$, mediated by the remaining colloidal particles. Here $\bar{\rho}=N/V$ is the number density of colloidal particles and g_3 is the three-particle correlation function, which is defined similarly to the pair-correlation function in Eq. (4) as

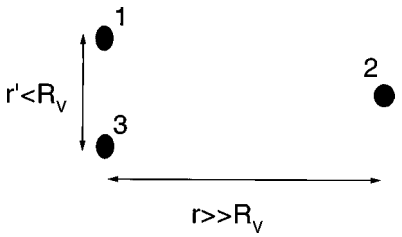

FIG. 2. Typical configuration for which a closure relation for the three-particle correlation function is needed. Particles 1 and 3 are separated to within a distance at most equal to the range R_V of the pair-interaction potential, while the distance between particles 1 and 3 and particle 2 is much larger than R_V.

$$g_3(\mathbf{r}_1,\mathbf{r}_2,\mathbf{r}_3,t)=V^3\int d\mathbf{r}_4\cdots\int d\mathbf{r}_N \times P(\mathbf{r}_1,\mathbf{r}_2,\mathbf{r}_3,\mathbf{r}_4,\ldots,\mathbf{r}_N,t). \quad (7)$$

Notice that since the equation of motion (5) is invariant under inversion (where $\mathbf{r}_j\rightarrow-\mathbf{r}_j$), the pair-correlation function is an even function, i.e., $g(\mathbf{r},t)=g(-\mathbf{r},t)$. To obtain a closed equation of motion we have to express the three-particle correlation function g_3 in Eq. (6) in terms of pair-correlation functions. The most commonly used, and for many purposes quite accurate closure, is the superposition approximation

$$\begin{aligned} g_3(\mathbf{r},\mathbf{r}',t)&\equiv g_3(\mathbf{r}_1-\mathbf{r}_2,\mathbf{r}_1-\mathbf{r}_3,t)\\ &=g(\mathbf{r}_1-\mathbf{r}_2,t)g(\mathbf{r}_2-\mathbf{r}_3,t)g(\mathbf{r}_1-\mathbf{r}_3,t)\\ &\equiv g(\mathbf{r},t)g(\mathbf{r}'-\mathbf{r},t)g(\mathbf{r}',t). \end{aligned} \quad (8)$$

This closure assumes pairwise independent pair correlations, thus neglecting the effect of a third particle on the correlation between two other particles. Close to the critical point this approximation can be improved. Actually, as was pointed out by Fixman [17], the improvement we are going to discuss is necessary in order to obtain a divergent correlation length at the critical point. The superposition approximation (8) as it stands is a poor approximation close to the critical point (and also close to the off-critical part of the spinodal). A closure relation is needed for distances $\mathbf{r}'=\mathbf{r}_1-\mathbf{r}_3$, which are equal to or smaller than the range R_V of the pair-interaction potential since in the integral in Eq. (6) $\nabla_{r'}V(r')=\mathbf{0}$ for distances $r'>R_V$. On the other hand, we are interested here only in the long-range behavior of the pair-correlation function since long-range correlations are responsible for the critical behavior of the suspension. Our interest is thus in the asymptotic solution of the equation of motion (5) for distances $r=|\mathbf{r}_1-\mathbf{r}_2|\gg R_V$. A typical configuration of particles for which a closure relation is needed is shown in Fig. 2. The neighboring particles 1 and 3 are to within a distance R_V from each other, while the particles 1 and 3 are separated from particle 2 by a distance large compared to R_V. The effect of the distant particle 2 is that it enhances the density around particles 1 and 3 since for these large distances the pair-correlation function is a smooth function of the distance. Therefore, the effect of particle 2 on the correlation between the neighboring particles 1 and 3 can, for our purpose, be described by taking into account a number density enhancement around particles 1 and 3. This density enhancement due to the presence of particle 2 is equal to $\bar{\rho}h(\mathbf{r}_2-(\mathbf{r}_1+\mathbf{r}_3)/2,t)=\bar{\rho}\mathbf{h}(\mathbf{r}-\frac{1}{2}\mathbf{r}',t)$, where $h=g-1$ is the total-correlation function. The pair-correlation function $g(\mathbf{r}_1-\mathbf{r}_3,t)=\mathbf{g}(\mathbf{r}',t)$ in Eq. (8) should therefore be evaluated at the enhanced density $\bar{\rho}+\bar{\rho}h(\mathbf{r}-\frac{1}{2}\mathbf{r}',t)$. Furthermore, since our interest here is in the asymptotic behavior of the pair-correlation function $g(\mathbf{r},t)$ for large distances $r\gg R_V$ and $h(\mathbf{r},t)\rightarrow0$ for $r\rightarrow\infty$, the equation of motion can be linearized with respect to $h(\mathbf{r}-\mathbf{r}',t)$ and $h(\mathbf{r}-\frac{1}{2}\mathbf{r}',t)$. The linearized form of the pair-correlation function $g(\mathbf{r}')$ at the enhanced density reads

$$g(\mathbf{r}',t)|_{\text{at the enhanced density}}=g(\mathbf{r}',t)+\frac{dg(\mathbf{r}',t)}{d\bar{\rho}}\bar{\rho}h(\mathbf{r}-\tfrac{1}{2}\mathbf{r}',t), \quad (9)$$

where the correlation functions on the right-hand side refer to the system with particle number density $\bar{\rho}$. Substitution of Eqs. (8) and (9) into the equation of motion (5) and further linearization with respect to h yields

$$\begin{aligned} \frac{\partial h(\mathbf{r},t)}{\partial t}=2D_0\nabla_r\cdot\Bigg[&\nabla_r h(\mathbf{r},t)+\beta\{h(\mathbf{r},t)+1\}\Bigg([\nabla_r V(r)]\\ &+\bar{\rho}\int d\mathbf{r}'[\nabla_{r'}V(r')]g(\mathbf{r}',t)\Bigg)\\ &+\beta\bar{\rho}\int d\mathbf{r}'[\nabla_{r'}V(r')]\Bigg(g(\mathbf{r}',t)h(\mathbf{r}-\mathbf{r}',t)\\ &+\frac{dg(\mathbf{r}',t)}{d\bar{\rho}}\bar{\rho}h\Big(\mathbf{r}-\frac{1}{2}\mathbf{r}',t\Big)\Bigg)\Bigg]-\nabla_r\cdot[\boldsymbol{\Gamma}\cdot\mathbf{r}h(\mathbf{r},t)]. \end{aligned} \quad (10)$$

For $r\gg R_V$ and $r'<R_V$, both $h(\mathbf{r}-\mathbf{r}')$ and $h(\mathbf{r}-\frac{1}{2}\mathbf{r}')$ are smooth functions of $\mathbf{r}'$ on the length scale R_V, which can therefore be Taylor expanded as

$$\begin{aligned} h(\mathbf{r}-\mathbf{r}',t)=&h(\mathbf{r},t)-\mathbf{r}'\cdot\nabla_r h(\mathbf{r},t)+\tfrac{1}{2}\mathbf{r}'\mathbf{r}':\nabla_r\nabla_r h(\mathbf{r},t)\\ &-\tfrac{1}{6}\mathbf{r}'\mathbf{r}'\mathbf{r}'\vdots\nabla_r\nabla_r\nabla_r h(\mathbf{r},t)\cdots,\\ h(\mathbf{r}-\tfrac{1}{2}\mathbf{r}',t)=&h(\mathbf{r},t)-\tfrac{1}{2}\mathbf{r}'\cdot\nabla_r h(\mathbf{r},t)+\tfrac{1}{8}\mathbf{r}'\mathbf{r}':\nabla_r\nabla_r h(\mathbf{r},t)\\ &-\tfrac{1}{48}\mathbf{r}'\mathbf{r}'\mathbf{r}'\vdots\nabla_r\nabla_r\nabla_r h(\mathbf{r},t)\cdots. \end{aligned}$$

Furthermore, since the interest here is in the distortion of long-range correlations, we neglect the shear induced distortions of short-range correlations: long range correlations are much more sensitive to shear flow than short-range correlations because at short distances shear forces are smaller and the counterbalancing, equilibrium restoring interactions are stronger. The amount of distortion of correlations with a range R_V or less is measured by the bare Péclet number $\mathrm{Pe}^0=\dot{\gamma}R_V^2/2D_0$ for the stationary shear flow and $\mathrm{Pe}_s^0=\dot{\gamma}_sR_V^2/2D_0$ for the superimposed oscillatory shear component of the fluid flow. The shear rates are supposed to be small enough that these bare Péclet numbers are small [18].

The pair-correlation function $g(\mathbf{r}',t)$ in the above integrals is therefore set equal to the equilibrium pair-correlation function $g^{eq}(r')$, that is, the pair-correlation function in the absence of shear flow. Substitution of the above Taylor expansions into Eq. (10) and performing angular integrations leads to

$$\frac{\partial h(\mathbf{r},t)}{\partial t}=D_0\nabla_r\cdot\left\{\beta\{h(\mathbf{r},t)+1\}[\nabla_r V(r)]+\beta\frac{d\Pi}{d\bar{\rho}}\nabla_r h(\mathbf{r},t)-\beta\Sigma\nabla_r\nabla_r^2 h(\mathbf{r},t)\right\}-\nabla_r\cdot[\mathbf{\Gamma}\cdot\mathbf{r}h(\mathbf{r},t)], \tag{11}$$

where

$$\Pi=\bar{\rho}k_BT-\frac{2\pi}{3}\bar{\rho}^2\int_0^\infty dr'r'^3\frac{dV(r')}{dr'}g^{\mathrm{eq}}(r') \tag{12}$$

is precisely the osmotic pressure of the suspension and

$$\Sigma=\frac{2\pi}{15}\bar{\rho}\int_0^\infty dr'r'^5\frac{dV(r')}{dr'}\left\{g^{\mathrm{eq}}(r')+\frac{1}{8}\bar{\rho}\frac{dg^{eq}(r')}{d\bar{\rho}}\right\} \tag{13}$$

is a positive constant, proportional to the Cahn-Hilliard square gradient coefficient. A Fourier transformation of Eq. (11) and subtraction of the equation without shear flow, using Eq. (2) for the velocity gradient matrix, yields

$$\frac{\partial S(\mathbf{k},t)}{\partial t}=[\dot{\gamma}k_1+\dot{\gamma}_s\cos\{\omega t\}k_3]\frac{\partial S(\mathbf{k},t)}{\partial k_2}-2D^{\mathrm{eff}}(k)k^2\{S(\mathbf{k},t)-S^{\mathrm{eq}}(k)\}, \tag{14}$$

where k_j is the jth component of the wave vector $\mathbf{k}$ and

$$S(\mathbf{k},t)=1+\bar{\rho}\int d\mathbf{r}h(\mathbf{r},t)\exp\{-i\mathbf{k}\cdot\mathbf{r}\} \tag{15}$$

is the static structure factor, while S^{eq} is the structure factor without shear flow. Furthermore $D^{\mathrm{eff}}(k)$ is a wave-vector-dependent effective diffusion coefficient equal to

$$D^{\mathrm{eff}}(k)=D_0\beta\left[\frac{d\Pi}{d\bar{\rho}}+k^2\Sigma\right]. \tag{16}$$

The first term on the right-hand side of Eq. (14) describes shear flow distortion, while the last term describes the diffusion limited tendency to restore the equilibrium microstructure. Close to the critical point (and also close to the off-critical part of the spinodal), where $\beta d\Pi/d\bar{\rho}$ is small, the effective diffusion coefficient is small for small wave vectors, a phenomenon that is commonly referred to as critical slowing down.

As we will show, the general solution of the equation of motion (14) can be expressed in terms of explicit expressions for structure factors for two more simple cases: the structure factor in the absence of shear flow S^{eq} and under stationary shear flow S^{stat}, in the absence of the oscillatory shear flow. These two more simple cases will be considered in the following, before solving the full equation of motion (14).

The above equations relate to the mean-field behavior of the structure factor. This is due to linearization of the equation of motion (5) with respect to the total-correlation function h. On linearization, terms of order h^2 are neglected against the important linear term $h\beta d\Pi/d\bar{\rho}$. Very close to the critical point, where $\beta d\Pi/d\bar{\rho}$ is a very small number, the nonlinear terms become equally important as the mentioned linear term. Beyond the mean-field region one has to solve nonlinear equations of motion. Such nonlinear equations are not considered in the present paper.

It is important to realize that the shear induced shift of the spinodal and the critical point is related to the distortion of correlations over distances less than the range R_V of the pair-interaction potential [19]. These short-range distortions are neglected in deriving the above equation of motion and therefore the shift of the critical point playes no role here. Notice, however, that a very small shift of the critical point in the phase diagram is unimportant only when that shift is much smaller than the distance of the unsheared system to the critical point. Since we restrict ourselves here to the mean-field region it is probably safe to neglect the small, shear induced shift of the critical point.

B. Equilibrium structure factor $S^{\mathrm{eq}}(k)$

The equilibrium structure factor S^{eq} can be calculated from the stationary form of the equation of motion (11), which reduces without shear and for $r\gg R_V$, where $\nabla_r V(r)=\mathbf{0}$, to

$$\Sigma\nabla_r^2 h^{\mathrm{eq}}(r)=\frac{d\Pi}{d\bar{\rho}}h^{\mathrm{eq}}(r). \tag{17}$$

The solution of this equation is the well-known Ornstein-Zernike total-correlation function

$$h^{\mathrm{eq}}(r)=(AR_V)\frac{\exp\{-r/\xi\}}{r}, \tag{18}$$

where the correlation length ξ is equal to

$$\xi=\sqrt{\Sigma\Big/\frac{d\Pi}{d\bar{\rho}}} \tag{19}$$

and A is a dimensionless integration constant. The relevance of the correlation length is that it measures the range over which colloidal particles in the unsheared system are correlated. Since $d\Pi/d\bar{\rho}\to 0$ on approach of the critical point (and also on approach of the off-critical part of the spinodal), the correlation length diverges. This means that at the critical point each colloidal particle in the system is correlated with all other colloidal particles. One may imagine that it will take an infinite force to break up these many correlations in order to make the system flow, which means that the viscosity diverges on approach of the spinodal.

Substitution of Eq. (18) into the defining expression (15) for the structure factor gives

$$S^{\mathrm{eq}}(k)=1+4\pi\bar{\rho}(AR_V)\frac{1}{\xi^{-2}+k^2}. \tag{20}$$

Since at $k=0$ the equilibrium structure factor is equal to $k_BT/(d\Pi/d\overline{\rho})$, it follows that the integration constant is equal to

$$AR_V=\frac{1}{4\pi\overline{\rho}}\frac{1}{\xi^2}\left\{\left[\beta\frac{d\Pi}{d\overline{\rho}}\right]^{-1}-1\right\}.$$

Substitution into Eq. (20) gives

$$S^{\mathrm{eq}}(k)=\frac{(\beta\Sigma)^{-1}\xi^2+(k\xi)^2}{1+(k\xi)^2}. \tag{21}$$

In the neighborhood of the critical point $\beta\Sigma$ is estimated from Eqs. (12) and (13) to be of the order R_V^2 [20]. In addition, the above equations are valid only for small wave vectors $k\ll 2\pi/R_V$, so that Eq. (21) reduces to

$$S^{\mathrm{eq}}(k)=\frac{1}{\beta\Sigma}\frac{\xi^2}{1+(k\xi)^2}, \tag{22}$$

which is the well-known Ornstein-Zernike structure factor [21].

C. Dimensionless form of the equation of motion

With Eq. (19) for the correlation length and Eq. (16) for the effective diffusion coefficient, the equation of motion (14) can be written more elegantly in a dimensionless form by introducing the dimensionless wave vector

$$\mathbf{K}=\mathbf{k}\xi \tag{23}$$

and the dimensionless time

$$\tau=2D^{\mathrm{eff}}(k=0)\xi^{-2}t=2D_0\beta\Sigma\,\xi^{-4}t. \tag{24}$$

The dimensionless equation of motion (14) reads

$$\frac{\partial S(\mathbf{K},\tau)}{\partial\tau}=[\lambda K_1+\lambda_s\cos\{\Omega\tau\}K_3]\frac{\partial S(\mathbf{K},\tau)}{\partial K_2}-K^2[1+K^2]\times\{S(\mathbf{K},\tau)-S^{\mathrm{eq}}(K)\}, \tag{25}$$

where the following ''dressed Péclet numbers'' are introduced:

$$\lambda=\frac{\dot\gamma\xi^4}{2D_0\beta\Sigma}=\frac{\dot\gamma\xi^2}{2D^{\mathrm{eff}}(k=0)},\quad \lambda_s=\frac{\dot\gamma_s\xi^4}{2D_0\beta\Sigma}=\frac{\dot\gamma_s\xi^2}{2D^{\mathrm{eff}}(k=0)}, \tag{26}$$

and Ω is a dimensionless frequency (or a dressed Deborah number),

$$\Omega=\frac{\omega\xi^4}{2D_0\beta\Sigma}=\frac{\omega\xi^2}{2D^{\mathrm{eff}}(k=0)}. \tag{27}$$

The dimensionless numbers λ and λ_s measure the long-wavelength shear induced distortion of the structure factor. The crossover from the weak shear regime, where shear effects are small, to the strong shear regime, where shear effects are significant, occurs at $\lambda\approx 1$ for the stationary shear flow and at $\lambda_s\approx 1$ for the superimposed oscillatory component of the flow. A significant phase shift of the structure factor response relative to the external field $\sim\cos\{\omega t\}$ will be found for $\Omega>1$, while for $\Omega<1$ the viscous response will be almost instantaneous. Notice that λ, λ_s, and Ω, for given $\dot\gamma$, $\dot\gamma_s$, and ω, become larger on approach of the critical point because of the increasing correlation length ξ. The effect of shear flow for given shear rates $\dot\gamma$ and $\dot\gamma_s$ is thus more pronounced closer to the critical point. This is due to the increasing size ξ of ''clusters of correlated particles'' on approach of the critical point since larger clusters are more easily affected by shear flow. Furthermore, the dynamics of these larger clusters is slow so that the typical frequency ω where the response of the structure factor will have an out-of-phase component with the applied field occurs at smaller frequencies.

D. Stationary sheared structure factor $S^{\mathrm{stat}}(\mathbf{k})(\dot\gamma_s=0)$

Let us consider the relatively simple case of a stationary shear flow, where $\dot\gamma_s=0$ [16]. The dimensionless equation of motion reduces for this case to

$$0=\lambda K_1\frac{\partial S^{\mathrm{stat}}(\mathbf{K})}{\partial K_2}-K^2[1+K^2]\{S^{\mathrm{stat}}(\mathbf{K})-S^{\mathrm{eq}}(K)\}. \tag{28}$$

The solution of this equation of motion can be obtained by integration with respect to K_2. The solution is constructed in Appendix A, where the δ-distribution representation (A1) plays an essential role. The following expression for the Ornstein-Zernike structure factor under stationary shear flow is found:

$$S^{\mathrm{stat}}(\mathbf{K})=S^{\mathrm{eq}}(K)\left[1+\frac{1}{\lambda K_1}\int_{K_2}^{\pm\infty}dX[K^2-K_2^2+X^2]\times[K_2^2-X^2]\exp\left\{-\frac{F(\mathbf{K}|X)}{\lambda K_1}\right\}\right], \tag{29}$$

where S^{eq} is given by Eq. (22) and

$$F(\mathbf{K}|X)=\int_{K_2}^{X}dY[K^2-K_2^2+Y^2][1+K^2-K_2^2+Y^2]=[X-K_2][K^2-K_2^2][1+K^2-K_2^2]+\frac{1}{3}[X^3-K_2^3][1+2K^2-2K_2^2]+\frac{1}{5}[X^5-K_2^5]. \tag{30}$$

The upper integration limit in Eq. (29) is equal to $+\infty$ when $\lambda K_1>0$ and equal to $-\infty$ when $\lambda K_1<0$. As can be seen from Eq. (28), for $\lambda=0$ and/or $K_1=0$, the stationary structure factor becomes equal to the equilibrium structure factor. That the solution in Eq. (29) satisfies this requirement is shown in Appendix A. Perpendicular to the flow direction, where $K_1=0$, there is thus no effect of shear flow and $S^{\mathrm{stat}}=S^{\mathrm{eq}}$. Distortions in directions where $K_1=0$ may occur beyond mean-field, where instead of the linear equation of motion (28) a nonlinear equation should be considered. In addition, such distortions may result from hydrodynamic interactions, which are neglected in the present theory, or

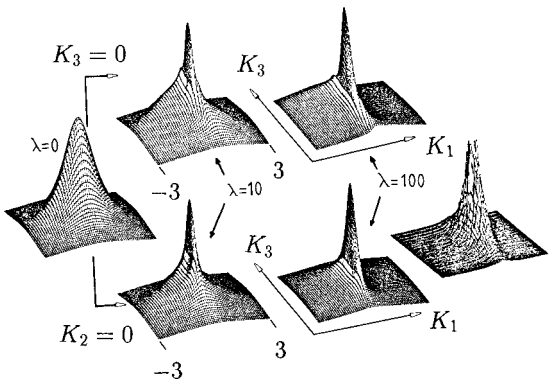

FIG. 3. Static structure factor as a function of K_1 and K_2 with $K_3=0$ (upper figures) and of K_1 and K_3 with $K_2=0$ (lower figures), for $\lambda=10$ and 100. The leftmost figure is the equilibrium Ornstein-Zernike static structure factor. A value of 1/100 is chosen for the quantity $(R_V/\xi)^2(\beta\Sigma/R_V^2)$. The rightmost figure is an experimental scattering pattern (with $K_2=0$).

may be the result of distortions of short-range correlations that couple to the long-range structure. The shear rates are assumed here to be small enough to be able to neglect these short-range distortions. Short-range correlations are not affected by the stationary shear flow when the ''bare Péclet number'' $\mathrm{Pe}^0=\dot\gamma R_V^2/2D_0$ is small [18]. Since $\xi\gg R_V$ and $D^{\mathrm{eff}}(k=0)\ll D_0$, λ can be a large number while at the same shear rate Pe^0 is a small number. Hence large-scale structures are already severely affected by shear flow at shear rates where small-scale structures are virtually unaffected. Figure 3 shows the highly anisotropic microstructure under shear flow for various values of the dimensionless shear rate λ. For comparison, the rightmost figure is an experimental result.

E. Structure factor under orthogonally superimposed shear flow

The structure factor under an oscillatory shear flow, orthogonally superimposed onto a stationary shear flow, will be an alternating function of time around the stationary structure factor as given in Eq. (29). To obtain this alternating solution it is more convenient to start from an equation of motion for the difference

$$\Delta S(\mathbf{K},\tau)\equiv S(\mathbf{K},\tau)-S^{\mathrm{stat}}(\mathbf{K}). \tag{31}$$

From Eqs. (25) and (28) one obtains the equation of motion for this difference

$$\frac{\partial\Delta S(\mathbf{K},\tau)}{\partial\tau}=[\lambda K_1+\lambda_s\cos\{\Omega\tau\}K_3]\frac{\partial\Delta S(\mathbf{K},\tau)}{\partial K_2}-K^2[1+K^2]\Delta S(\mathbf{K},\tau)+\frac{\lambda_s K_3}{\lambda K_1}K^2[1+K^2]\times\cos\{\Omega\tau\}\{S^{\mathrm{stat}}(\mathbf{K})-S^{\mathrm{eq}}(K)\}. \tag{32}$$

The solution of this equation of motion is constructed in Appendix B. The alternating solution, after transients died out, reads

$$S(\mathbf{K},\tau)=S^{\mathrm{stat}}(\mathbf{K})+\frac{\lambda_s K_3}{\lambda K_1}\int_{-\infty}^{\tau}d\tau'\cos\{\Omega\tau'\}G^2(\tau')\times[1+G^2(\tau')]\{S^{\mathrm{stat}}(\mathbf{G}(\tau'))-S^{\mathrm{eq}}(G(\tau'))\}\times\exp\{-H(\tau')\}, \tag{33}$$

where the vector $\mathbf{G}$ is equal to

$$\mathbf{G}(\tau')=\left(K_1,K_2+\lambda K_1(\tau-\tau')+\frac{\lambda_s K_3}{\Omega}[\sin\{\Omega\tau\}-\sin\{\Omega\tau'\}],K_3\right), \tag{34}$$

$G(\tau')$ is its length and the function $H(\tau')$ in the exponent is equal to

$$H(\tau')=\int_{\tau'}^{\tau}d\tau''G^2(\tau'')[1+G^2(\tau'')]. \tag{35}$$

The latter integral can be done analytically with some effort. Nothing is learned from this very long explicit expression for H and therefore it is not displayed here. Notice that both $\mathbf{G}(\tau')$ and $H(\tau')$ are functions of τ and $\mathbf{K}$ as well.

A few features about the above expression for the structure factor are to be noted.

(i) The time dependence of the microstructure does not instantaneously follow that of the applied flow field ($\sim\cos\{\Omega\tau\}$). There is in general a phase shift between the response of the microstructure and the applied field, as a result of the finite diffusivity of the colloidal particles. This is illustrated in Fig. 4(a), where $-\Delta S=S^{\mathrm{stat}}-S$ is plotted as a function of $\Omega\tau$ for a wave vector equal to $\mathbf{K}=(1/\sqrt{3},1/\sqrt{3},1/\sqrt{3})$ and for three choices of the applied frequency $\Omega=0.1$, 1, and 10. For this wavevector a higher shear rate leads to a decrease of the structure factor, so that $-\Delta S$ will be in phase with the external field for low frequencies. The dimensionless shear rates λ and λ_s are taken equal to 1 and 0.1, respectively. The response $-\Delta S$ is scaled with its minimum or maximum value so as to limit its values to the interval $[-1,1]$. As can be seen, for a small value of $\lambda_s=0.1$, the microstructural response is almost linear in the applied field. The crossover from a linear to a nonlinear response occurs at $\lambda_s\approx 1$. The time lag of the microstructure with respect to the applied field becomes significant for $\Omega\approx 1$. This phase shift gives rise to an elastic component of the viscous reponse.

With increasing frequencies Ω the response ΔS, i.e., the oscillatory shear induced additional distortion, becomes smaller as the microstructure is not able to respond fast enough to the rapidly varying external field. Note that in Fig. 4(a) the response is scaled with respect to its maximum or minimum value, so that this decrease of ΔS with increasing frequency is not visible in that figure.

(ii) As can be seen from Fig. 4(b), the time dependence of the structure factor is not sinusoidal, like the applied field, when λ_s becomes larger than 1. This is due to the nonlinear dependence of the structure factor on the applied oscillatory shear rate $\lambda_s\cos\{\Omega\tau\}$. Higher-order Fourier components become relevant at larger λ_s, but they disappear again at larger applied frequencies. The nonlinear effects seem to become

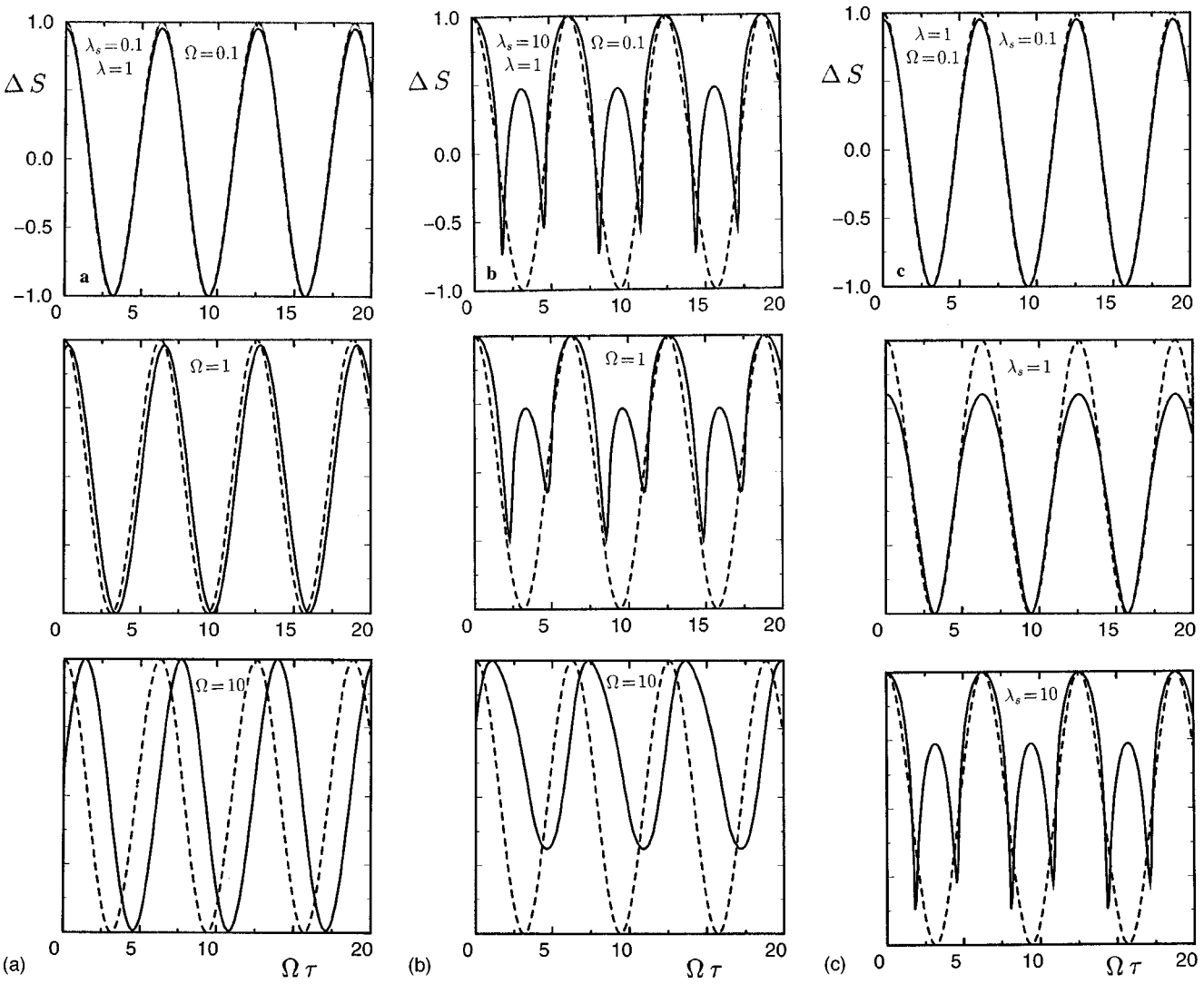

FIG. 4. External field (dashed line) and the temporal response of the normalized structure factor for the wave vector $\mathbf{K}=(1/\sqrt{3},1/\sqrt{3},1/\sqrt{3})$ (solid lines). The dimensionless shear rate for the stationary shear flow in these figures is $\lambda=1$. (a) The linear response regime ($\lambda_s=0.1$) with increasing frequency. (b) Nonlinear response regime ($\lambda_s=10$) with increasing frequency. (c) Low frequency ($\Omega=0.1$) with increasing oscillatory shear amplitude.

less pronounced at larger frequencies. The transition from a linear response to a nonlinear response is most clearly seen in Fig. 4(c), where λ_s is increased from top to bottom from 0.1 to 1 up to 10.

(iii) In Eq. (33) the dimensionless shear amplitude λ_s appears always as a product with K_3. This implies that in directions where $K_3=0$ there is no effect on the stationary sheared microstructure. Directions corresponding to $K_3=0$ are directions perpendicular to the oscillatory shear flow. A little thought shows that the morphology of density waves extending in these directions is indeed unaffected by the straining motion induced by the oscillatory flow. Oscillatory shear induced distortions in directions where $K_3=0$ could become important when the oscillatory shear rate $\dot{\gamma}_s$ is so large that short-range correlations are also affected. This will be the case when the bare Péclet number $\mathrm{Pe}_s^0=\dot{\gamma}_s R_V^2/2D_0$ corresponding to the oscillatory shear flow is larger than 1. The above expressions are valid when this bare Péclet number is smaller than 1 [18]. The same comments hold for the stationary structure factor in Eq. (29), where $K_1=0$ is the direction perpendicular to the stationary flow, and the relevant bare Péclet number is $\mathrm{Pe}^0=\dot{\gamma}R_V^2/2D_0$. Distortions perpendicular to a flow direction can also be the result of hydrodynamic interactions between the colloidal particles, which are neglected in the present theory. Furthermore, such distortions may become relevant beyond the mean-field region, even for small bare Péclet numbers and without a hydrodynamic interaction. Beyond the mean-field region nonlinear equations of motion should be considered, which may give rise to relevant distortions perpendicular to the flow direction.

(iv) At first sight it may seem that there is a divergence in the expressions (29) and (33) for S^{stat} and ΔS, respectively, in the case $\lambda K_1\to 0$. However, for $\lambda=0$ and/or $K_1=0$ one has $S^{\mathrm{stat}}=S^{\mathrm{eq}}$, as explained in the previous note (iii) and, in mathematical terms, at the end of Appendix A.

F. Structure factor under pure oscillatory shear flow ($\lambda=0$)

Consider the case of a purely oscillatory shear flow, where the stationary shear component is absent, i.e., $\dot{\gamma}=0$

$=\lambda$. The structure factor now reduces to the equilibrium structure factor when $\dot{\gamma}_s=0$ instead of the stationary structure factor as in Sec. III E. The equation of motion (25), now for $\Delta S\equiv S-S^{\rm eq}$, reads

$$\frac{\partial \Delta S(\mathbf{K},\tau)}{\partial \tau}=\lambda_s\cos\{\Omega\tau\}K_3\frac{\partial \Delta S(\mathbf{K},\tau)}{\partial K_2}-K^2[1+K^2]\times\Delta S(\mathbf{K},\tau)+\lambda_s\cos\{\Omega\tau\}K_3\frac{\partial S^{\rm eq}(K)}{\partial K_2}. \quad (36)$$

This equation of motion can be solved in exactly the same way as Eq. (32). Following the steps outlined in Appendix B, we obtain

$$S(\mathbf{K},\tau)=S^{\rm eq}(K)-2\lambda_s K_3\int_{-\infty}^{\tau}d\tau'\cos\{\Omega\tau'\}\frac{S^{\rm eq}(G_0(\tau'))}{1+G_0^2(\tau')}\times\left[K_2+\frac{\lambda_s K_3}{\Omega}(\sin\{\Omega\tau\}-\sin\{\Omega\tau'\})\right]\times\exp\{-H_0(\tau')\}, \quad (37)$$

with $S^{\rm eq}$ given by Eq. (22). The function $H_0(\tau')$ in the exponent is equal to

$$H_0(\tau')=\int_{\tau'}^{\tau}d\tau''G_0^2(\tau'')[1+G_0^2(\tau'')], \quad (38)$$

where G_0 is the length of the vector

$$\mathbf{G}_0(\tau')=\left(K_1,K_2+\frac{\lambda_s K_3}{\Omega}[\sin\{\Omega\tau\}-\sin\{\Omega\tau'\}],K_3\right). \quad (39)$$

The index 0 refers to the zero value of the stationary shear rate $\dot{\gamma}$.

An alternative route to arrive at this expression is to evaluate $S^{\rm stat}(\mathbf{G}(\tau'))-S^{\rm eq}(G(\tau'))$ in the integrand in Eq. (33) to linear order in λ using Eq. (28). It should be noticed that such a linear expansion is valid only when considering the limiting expression for $\dot{\gamma}\to 0$ since Eq. (28) is singularly perturbed by the stationary shear flow.

The above result simplifies considerably in the linear response regime. Since the integral in Eq. (37) is multiplied by λ_s, the linear response result is obtained by setting $\lambda_s=0$ in $\mathbf{G}_0$. Since for $\lambda_s=0$ we have $\mathbf{G}_0=\mathbf{K}$, Eq. (37) is easily seen to reduce to

$$S(\mathbf{K},\tau)=S^{\rm eq}(K)\left[1-\frac{2\lambda_s K_2K_3}{1+K^2}\int_{-\infty}^{\tau}d\tau'\cos\{\Omega\tau'\}\exp\{-(\tau-\tau')K^2(1+K^2)\}\right]=S^{\rm eq}(K)\left[1-\frac{2\lambda_s K_2K_3[K^2(1+K^2)\cos\{\Omega\tau\}+\Omega\sin\{\Omega\tau\}]}{(1+K^2)[\Omega^2+K^4(1+K^2)^2]}\right]. \quad (40)$$

This result can also be obtained from a linear response analysis of the equation of motion (36). The linear response result makes sense only when used to calculate viscoelastic response functions in the linear response regime. The equation of motion (36) is singularly perturbed with a boundary layer of width $\sim\sqrt{\lambda_s}$ around $\mathbf{K}=\mathbf{0}$. In this boundary layer the linear reponse expression (40) is invalid. For vanishing λ_s the width of the boundary layer vanishes and therefore does not contribute to wave vector integrals representing viscoelastic response functions.

The above expression for the structure factor under shear flow can be used to predict the dynamic viscous response of a near-critical suspension once a microscopic expression for the viscosity is derived. This is the subject of the subsequent section.

IV. MICROSCOPIC EXPRESSION FOR THE ANOMALOUS VISCOELASTIC RESPONSE FUNCTIONS

The range of correlations ξ is large close to the critical point and ultimately diverges. This implies that close to the critical point many colloidal particles interact simultaneously and at the critical point each colloidal particle interacts with all other colloidal particles in the system. This is the mechanism that leads to very large and ultimately infinite forces that are required to induce relative displacements of colloidal particles, corresponding to a large and ultimately diverging shear viscosity. In addition, the dynamics slows down considerably on approach of the critical point, leading to a dramatically changing dynamic viscous response of the system. We have to find a microscopic expression for the viscosity in order to quantitatively predict this anomalous behavior as the result of the development of long-range correlations.

Batchelor [22] derived a microscopic expression for the effective stress of suspensions that is valid for arbitrary concentrations and frequencies (not exceeding the inverse of the viscous relaxation time). Only a few terms in that expression are responsible for the anomalous behavior of the viscous response. The remaining terms contribute only to a well-behaved so-called background viscosity, which is the viscosity that would have been measured in the absence of the long-range correlations. In the following we shall rederive the term in Batchelor's expression that is responsible for anomalous behavior in a quite straighforward and elementary

way and revisit the definition of various viscoelastic response functions in the nonlinear regime.

First consider the linear viscoelastic response of the suspension. Let $\dot{U}$ be the rate at which energy is dissipated and stored per unit volume, due to the up-and-down oscillatory motion of the inner (or outer) cylinder. Let $F(t)$ denote the force that is applied to the oscillating cylinder in order to sustain a prescribed velocity $\dot{\gamma}_s\cos\{\omega t\}l$ relative to a stationary cylinder (where l is the gap width). The rate of energy dissipation and storage is $\dot{\gamma}_s\cos\{\omega t\}lF(t)$. In the linear regime the force is sinusoidal, like the velocity of the oscillating cylinder, but there may be a time lag between the two. The force $F(t)$ will therefore be of the form

$$F(t)/A=\dot{\gamma}_s[\,\eta'(\omega)\cos\{\omega t\}+\eta''(\omega)\sin\{\omega t\}], \tag{41}$$

with A the surface area of the oscillating cylinder. The in-phase viscosity $\eta'(\omega)$ and the out-of-phase viscosity $\eta''(\omega)$ thus describe the linear viscoelastic response of the suspension. For low frequencies, where $\Omega<1$, the microstructure will follow the applied field ($\sim\cos\{\omega t\}$) instantaneously, so that $\eta''(\omega=0)=0$. It thus follows that

$$\begin{aligned}\dot{U}&=\dot{\gamma}_s\cos\{\omega t\}lF(t)/lA\\&=\dot{\gamma}_s^2\cos\{\omega t\}[\,\eta'(\omega)\cos\{\omega t\}\\&\quad+\eta''(\omega)\sin\{\omega t\}].\end{aligned} \tag{42}$$

The in-phase viscosity $\eta'(\omega)$ measures the dissipated energy, while the out-of-phase component $\eta''(\omega)$ measures the elastically stored energy.

Let us extend the above result to the nonlinear regime. For larger shear rates $\dot{\gamma}_s$ the force $F(t)$ is an alternating function of time that is generally not sinusoidal, due to the nonlinear response of the microstructure, as depicted in Figs. 4(b) and 4(c). The alternating force $F(t)$, necessary to sustain the oscillatory motion of frequency ω, now exhibits higher-order frequencies. In this case the terms $\eta'(\omega)\cos\{\omega t\}$ and $\eta(\omega)''\sin\{\omega t\}$ in Eq. (42) should be replaced by a Fourier cosine and sine series, respectively, that is,

$$\eta'(\omega)\cos\{\omega t\}\rightarrow\sum_{n=1}^{\infty}\eta_n'(\omega)\cos\{n\omega t\}$$

and

$$\eta''(\omega)\sin\{\omega t\}\rightarrow\sum_{n=1}^{\infty}\eta_n''(\omega)\sin\{n\omega t\}.$$

In the linear response regime only $\eta_1'(\omega)$ and $\eta_1''(\omega)$ survive, which are then equal to $\eta'(\omega)$ and $\eta''(\omega)$, respectively. The linear response result (42) for the energy dissipation thus generalizes to

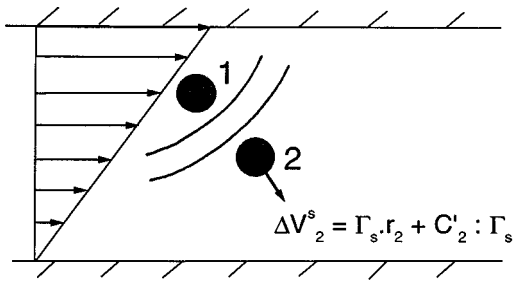

FIG. 5. Particle 2 experiences not only the incident shear field but also the flow field due to scattering of the shear field by the core of particle 1.

$$\begin{aligned}\dot{U}&=\dot{\gamma}_s\cos\{\omega t\}lF(t)/lA\\&=\dot{\gamma}_s^2\cos\{\omega t\}\sum_{n=1}^{\infty}[\,\eta_n'(\omega)\cos\{n\omega t\}\\&\quad+\eta_n''(\omega)\sin\{n\omega t\}].\end{aligned} \tag{43}$$

In an experiment in the nonlinear regime one often considers only the first few higher order Fourier components.

The dissipated and stored energy can also be expressed in terms of the hydrodynamic forces $\mathbf{F}_i^h$ that the fluid exerts on the colloidal particles $i=1,2\ldots,N$ and the *extra* velocity $\Delta\mathbf{V}_i^s$ that each particle attains as a result of the superimposed oscillatory shear field,

$$\dot{U}=\frac{1}{V}\sum_{i=1}^{N}\langle\Delta\mathbf{V}_i^s\cdot\mathbf{F}_i^h\rangle, \tag{44}$$

with V the volume of the system and angular brackets denoting ensemble averaging with respect to the shear-rate-dependent probability density function. Hence, from Eq. (43),

$$\begin{aligned}&\sum_{n=1}^{\infty}[\,\eta_n'(\omega)\cos\{n\omega t\}+\eta_n''(\omega)\sin\{n\omega t\}]\\&\quad=\frac{1}{\dot{\gamma}_s^2\cos\{\omega t\}V}\sum_{i=1}^{N}\langle\Delta\mathbf{V}_i^s\cdot\mathbf{F}_i^h\rangle.\end{aligned} \tag{45}$$

Let us denote the velocity gradient matrix corresponding to the flow induced by the superimposed oscillatory motion as $\mathbf{\Gamma}_s$, that is,

$$\mathbf{\Gamma}_s=\dot{\gamma}_s\cos\{\omega t\}\hat{\mathbf{\Gamma}}_s\quad\text{with}\quad\hat{\mathbf{\Gamma}}_s=\begin{pmatrix}0&0&0\\0&0&0\\0&1&0\end{pmatrix}. \tag{46}$$

The oscillatory shear induced velocity of a colloidal particle i is the local velocity of the fluid in the absence of colloidal particles $\mathbf{\Gamma}_s\cdot\mathbf{r}_i$, with $\mathbf{r}_i$ the position coordinate of the ith colloidal particle, plus a contribution due to the disturbance of the local fluid flow by the other colloidal particles. The incident flow field $\mathbf{\Gamma}_s\cdot\mathbf{r}$ is scattered by the cores of each of the colloidal particles, thereby affecting the motion of the other colloidal particles (see Fig. 5). This contribution is denoted as $\mathbf{C}_i':\mathbf{\Gamma}_s$. Hence

$$\Delta \mathbf{V}_i^s = \mathbf{\Gamma}_s \cdot \mathbf{r}_i + \mathbf{C}_i'(\mathbf{r}_1, \mathbf{r}_2, \ldots, \mathbf{r}_N) : \mathbf{\Gamma}_s . \tag{47}$$

The *disturbance matrices* $\mathbf{C}_j'$ of rank 3 are complicated functions of all the position coordinates of the colloidal particles. Leading-order terms in an expansion with respect to the inverse distance between the colloidal particles can be derived [23,16]. The way in which the ensemble average in Eq. (44) diverges on approach of the critical point is determined by the behavior of the phase function $\Delta \mathbf{V}_i^s \cdot \mathbf{F}_i^h$ at large distances. It is therefore sufficient to use the asymptotic form of $\mathbf{C}_j'$ at large distances. This asymptotic form is simply the first term in an expansion with respect to the inverse distances between colloidal particles, which is nothing but the expression for $\mathbf{C}_j'$ on the pair level. The higher-order many-body interaction contributions to $\mathbf{C}_j'$ vanish at infinity more rapidly than its two-particle contributions. Using the two-particle form of $\mathbf{C}_j'$ does not mean that one performs an expansion to leading order in the density, which would be completely wrong near the critical point. Instead, this two-particle form is the leading term for large distances, whose contribution determines the way in which viscoelastic response functions diverge. The disturbance matrix is now a sum of matrices $\mathbf{C}$ depending on just two position coordinates ($\mathbf{r}_{ij} = \mathbf{r}_i - \mathbf{r}_j$),

$$\mathbf{C}_i' = \sum_{j=1, j\neq i}^{N} \mathbf{C}(\mathbf{r}_{ij}). \tag{48}$$

For the evaluation of the effective viscosity we will need the explicit leading-order expression for the divergence of the vector $\mathbf{C}:\mathbf{\Gamma}_s$, which reads

$$\nabla_i \cdot [\mathbf{C}(\mathbf{r}_{ij}) : \mathbf{\Gamma}_s] = \frac{75}{2}\left(\frac{a}{r_{ij}}\right)^6 (\hat{\mathbf{r}}_{ij} \cdot \mathbf{\Gamma}_s \cdot \hat{\mathbf{r}}_{ij}), \tag{49}$$

where $\hat{\mathbf{r}}_{ij} = \mathbf{r}_{ij}/r_{ij}$ and a is the core radius of the spherical colloidal particles.

On the Smoluchowski time scale, the inertial force on each colloidal particle is negligibly small, so that the hydrodynamic forces $\mathbf{F}_i^h$ are equal to minus the sum of the direct force

$$\mathbf{F}_i^I = -\nabla_i \Phi \tag{50}$$

and the Brownian force

$$\mathbf{F}_i^{Br} = -k_B T \nabla_i \ln P, \tag{51}$$

with Φ the total potential energy of the colloidal particles and P the (shear-rate-dependent) probability density function of the position coordinates. In equilibrium, without shear flow, these two forces add up to zero, yielding the Boltzmann probability density function $P \sim \exp\{-\Phi/k_B T\}$. In a sheared system there is an unbalance between these two forces, so P is no longer equal to the Boltzmann exponential. This effect of shear flow on the pair-correlation function or, equivalently, on the structure factor, has been analyzed in Sec. III. The ensemble average in Eq. (45) is to be taken with respect to this shear-rate-dependent probability density function. Substitution of Eq. (47) for the oscillatory shear induced velocity and Eqs. (50) and (51) with $\mathbf{F}_i^h = -\mathbf{F}_i^I - \mathbf{F}_i^{\mathrm{Br}}$ for the hydrodynamic force into Eq. (45) gives

$$\sum_{n=1}^{\infty} [\eta_n'(\omega)\cos\{n\omega t\} + \eta_n''(\omega)\sin\{n\omega t\}] = \frac{1}{\dot{\gamma}_s V} \sum_{i=1}^{N} \langle (\hat{\mathbf{\Gamma}}_s \cdot \mathbf{r}_i + \mathbf{C}_i' : \hat{\mathbf{\Gamma}}_s) \cdot (\nabla_i \Phi + k_B T \nabla_i \ln P) \rangle. \tag{52}$$

There are further contributions to the viscosity that stem from direct interactions of solvent molecules with the colloidal particles, *the hydrodynamic viscosity*, and from interactions between solvent molecules. These contributions will not be considered here since they contribute only to the well-behaved background viscosity. Only the interactions between colloidal particles become long ranged upon approach of the critical point, while the other interactions remain short ranged and therefore do not contribute to the anomalous behavior of the effective viscosity.

The various viscoelastic response functions now follow from Eq. (52) as

$$\begin{Bmatrix} \eta_n'(\omega) \\ \eta_n''(\omega) \end{Bmatrix} = \frac{\omega}{\pi \dot{\gamma}_s V} \sum_{i=1}^{N} \int_0^{2\pi/\omega} dt \begin{Bmatrix} \cos\{n\omega t\} \\ \sin\{n\omega t\} \end{Bmatrix} \times \langle (\hat{\mathbf{\Gamma}}_s \cdot \mathbf{r}_i + \mathbf{C}_i' : \hat{\mathbf{\Gamma}}_s) \cdot (\nabla_i \Phi + k_B T \nabla_i \ln P) \rangle. \tag{53}$$

Using the expressions for the structure factor as derived in Sec. III, these microscopic expressions are evaluated explicitly in Sec. V. Numerical results are given in Secs. VI and VII.

In an experiment one typically measures the force $F(t)$ on the cylinder that is needed to sustain a prescribed velocity. According to Eq. (43), this force is equal to

$$F(t)/A = \dot{\gamma}_s \sum_{n=1}^{\infty} [\eta_n'(\omega)\cos\{n\omega t\} + \eta_n''(\omega)\sin\{n\omega t\}]. \tag{54}$$

The various viscoelastic response functions are therefore experimentally obtained from a Fourier series analysis as

$$\begin{Bmatrix} \eta_n'(\omega) \\ \eta_n''(\omega) \end{Bmatrix} = \frac{\omega}{\pi \dot{\gamma}_s} \int_0^{2\pi/\omega} dt \begin{Bmatrix} \cos\{n\omega t\} \\ \sin\{n\omega t\} \end{Bmatrix} F(t)/A. \tag{55}$$

These experimental data can then be compared to the theoretical predictions following from Eq. (53).

V. EVALUATION OF THE VISCOELASTIC RESPONSE FUNCTIONS

The quantity of interest in the microscopic expression (53) for the viscoelastic response functions is

$$N(t) \equiv \frac{1}{\dot{\gamma}_s V} \sum_{i=1}^{N} \langle (\hat{\mathbf{\Gamma}}_s \cdot \mathbf{r}_i + \mathbf{C}_i' : \hat{\mathbf{\Gamma}}_s) \cdot (\nabla_i \Phi + k_B T \nabla_i \ln P) \rangle. \tag{56}$$

For convenience this quantity is written as the sum of four terms

$$N(t) = N_C^{\Phi}(t) + N_r^{\Phi}(t) + N_C^{\mathrm{Br}}(t) + N_r^{\mathrm{Br}}(t), \tag{57}$$

with

$$N_C^{\Phi}(t)=\frac{1}{\dot\gamma_s V}\sum_{i=1}^{N}\langle(\mathbf{C}_i':\hat{\mathbf{\Gamma}}_s)\cdot\nabla_i\Phi\rangle,$$

$$N_r^{\Phi}(t)=\frac{1}{\dot\gamma_s V}\sum_{i=1}^{N}\langle(\hat{\mathbf{\Gamma}}_s\cdot\mathbf{r}_i)\cdot\nabla_i\Phi\rangle,$$

$$N_C^{\mathrm{Br}}(t)=\frac{1}{\dot\gamma_s V}\sum_{i=1}^{N}\langle(\mathbf{C}_i':\hat{\mathbf{\Gamma}}_s)\cdot k_BT\nabla_i\ln P_N\rangle,$$

$$N_r^{\mathrm{Br}}(t)=\frac{1}{\dot\gamma_s V}\sum_{i=1}^{N}\langle(\hat{\mathbf{\Gamma}}_s\cdot\mathbf{r}_i)\cdot k_BT\nabla_i\ln P_N\rangle, \tag{58}$$

where the superscripts Br and Φ refer to the Brownian and direct force terms respectively, and the subscripts C and r to the terms involving $\mathbf{C}_i'$ and $\hat{\mathbf{\Gamma}}_s\cdot\mathbf{r}_i$.

Most of the terms here probe the short range distortion of correlations, which do not contribute to the anomalous part of the response functions. These terms are regular functions of the bare Péclet number $\mathrm{Pe}_s^0=\dot\gamma_s R_V^2/2D_0$ that measures these short-range distortions. Such terms contribute only to the background viscosity, which is the viscosity that would have been measured in the absence of long-range correlations.

Let us consider each of the contributions to $N(t)$ in Eq. (57) separately. For convenience we shall not denote the time dependence of probability density functions in the following.

(i) The contribution $N_C^{\Phi}(t)$. Substitution of Eq. (48) for $\mathbf{C}_i'$, assuming a pairwise additive potential energy and identical colloidal particles, yields

$$N_C^{\Phi}(t)=\frac{\overline{\rho^2}}{\dot\gamma_s}\int d\mathbf{R}\,g(\mathbf{R})[\mathbf{C}(\mathbf{R}):\hat{\mathbf{\Gamma}}_s]\cdot\nabla_R V(R)+\frac{\overline{\rho^3}}{\dot\gamma_s}\int d\mathbf{r}\int d\mathbf{R}g_3(\mathbf{R},\mathbf{r})[\nabla_r V(r)]\cdot[\mathbf{C}(\mathbf{R}):\hat{\mathbf{\Gamma}}].$$

The first integral on the right-hand side probes the shear rate dependence of the short-range $\mathbf{r}$ dependence of the pair-correlation function since it is multiplied by $\nabla_r V(r)$. The first integral therefore does not contribute to the anomalous behavior of the viscosity. The second integral may be evaluated as follows. In order to separate the anomalous part from the background contribution, the total-correlation function is decomposed in a long-range and a short-range contribution h_l and h_s, respectively,

$$g(\mathbf{r})=1+h_l(\mathbf{r})+h_s(\mathbf{r}). \tag{59}$$

Formally, the long-range part h_l of the total-correlation function is defined as the asymptotic solution of the Smoluchowski equation for large distances as found in Sec. III. The remainder is the short-range part h_s, which is 0 for distances larger than a few times R_V. What is important is that the short-range part h_s does not contribute to the anomalous part of the viscosity since the anomalous behavior is the result of long-range correlations.

First of all, linearization with respect to the long-range contributions h_l is allowed since the total-correlation function goes to zero at infinity. After substitution of the decomposition (59) into the closure relation (8) and (9) for g_3, with $\mathbf{r}$ replaced by $\mathbf{R}$ and $\mathbf{r}'$ by $\mathbf{r}$, such a linearization leads to

$$N_C^{\Phi}(t)=\frac{\overline{\rho^3}}{\dot\gamma_s}\int d\mathbf{r}\int d\mathbf{R}[1+h_l(\mathbf{R}-\mathbf{r})+h_l(\mathbf{R})+\underline{h_l(\mathbf{R})h_s(\mathbf{R}-\mathbf{r})}+\underline{h_s(\mathbf{R}-\mathbf{r})}+\underline{h_s(\mathbf{R})h_l(\mathbf{R}-\mathbf{r})}+\underline{h_s(\mathbf{R})h_s(\mathbf{R}-\mathbf{r})}]\left\{g(\mathbf{r})+\frac{dg(\mathbf{r})}{d\overline{\rho}}\overline{\rho}\left[h_l\left(\mathbf{R}-\frac{1}{2}\mathbf{r}\right)+h_s\left(\mathbf{R}-\frac{1}{2}\mathbf{r}\right)\right]\right\}[\nabla_r V(r)]\cdot[\mathbf{C}(\mathbf{R}):\hat{\mathbf{\Gamma}}_s].$$

The underlined terms probe only the short-range distortion of the correlation functions and therefore do not contribute to the anomalous part of the viscosity. For example, the first underlined term $\sim h_s(\mathbf{R}-\mathbf{r})$ is only nonzero for $|\mathbf{R}-\mathbf{r}|$ smaller than a few times R_V. Since the factor $\nabla_r V(r)$ limits the integration range of $\mathbf{r}$ to $r\leqslant R_V$, this implies that the integration range of $\mathbf{R}$ is also limited to a few times R_V.

Second, since $r\leqslant R_V$, the correlation functions $h_l(\mathbf{R}-\mathbf{r})$ and $h_l(\mathbf{R}-\frac{1}{2}\mathbf{r})$ are smooth functions of $\mathbf{r}$ for large distances $\mathbf{R}$. These correlation functions may therefore be Taylor expanded to first order in gradients

$$h_l(\mathbf{R}-\mathbf{r})=h_l(\mathbf{R})-\mathbf{r}\cdot\nabla_R h_l(\mathbf{R}),$$

$$h_l(\mathbf{R}-\tfrac{1}{2}\mathbf{r})=h_l(\mathbf{R})-\tfrac{1}{2}\mathbf{r}\cdot\nabla_R h_l(\mathbf{R}).$$

Substitution of these expansions and a further linearization with respect to h_l yields

$$N_C^{\Phi}(t)=\frac{\overline{\rho^3}}{\dot\gamma_s}\int d\mathbf{r}\int d\mathbf{R}\left[g(\mathbf{r})(\underline{1+2h_l(\mathbf{R})}-\mathbf{r}\cdot\nabla_R h_l(\mathbf{R})]+\frac{dg(\mathbf{r})}{d\overline{\rho}}\overline{\rho}\left(\underline{h_l(\mathbf{R})}-\frac{1}{2}\mathbf{r}\cdot\nabla_R h_l(\mathbf{R})\right)\right]\times[\nabla_r V(r)]\cdot[\mathbf{C}(\mathbf{R}):\hat{\mathbf{\Gamma}}_s].$$

The underlined terms do not contribute upon integration since the corresponding integrand is an odd function of either $\mathbf{r}$ or $\mathbf{R}$ [note that both $\nabla_r V(r)$ and $\mathbf{C}(\mathbf{R})$ are odd functions]. Finally, $g(\mathbf{r})$ may be replaced by the equilibrium pair-correlation function $g^{\mathrm{eq}}(r)$ since it is multiplied in the integral by $\nabla_r V(r)$. The spherical angular integrations with respect to $\mathbf{r}$ can now be performed to yield

$$N_C^{\Phi}(t)=\frac{\overline{\rho^2}}{\dot\gamma_s}\left[\frac{d\Pi}{d\overline{\rho}}-k_BT\right]\int d\mathbf{R}[\mathbf{C}(\mathbf{R}):\hat{\mathbf{\Gamma}}_s]\cdot\nabla_R h_l(\mathbf{R}), \tag{60}$$

where Π is the osmotic pressure of the quiescent, unsheared suspension [see Eq. (12)]. Since the hydrodynamic interaction matrix $\mathbf{C}$ goes to zero as R^{-2} for $R\to\infty$, the above integral probes the long-range behavior of the total-correlation function and therefore may contribute to the anomalous behavior of the effective viscosity.

(ii) The contribution $N_r^{\Phi}(t)$. Using that the pair-interaction potential and the pair-correlation function are even functions and assuming again identical colloidal particles, it is found that

$$N_r^{\Phi}(t)=\frac{1}{2}\frac{\overline{\rho^2}}{\dot\gamma_s}\int d\mathbf{R}g(\mathbf{R})(\hat{\mathbf{\Gamma}}_s\cdot\mathbf{R})\cdot\nabla_R V(R). \tag{61}$$

Only the short-range behavior of $g(\mathbf{R})$ is probed here since g is multiplied in the integrand by $\nabla_R V(R)$. Therefore, $N_r^{\Phi}(t)$ does not contribute to the anomalous behavior.

(iii) The contribution $N_C^{Br}(t)$. In order to evaluate this contribution, we use the superposition approximation on the N-particle level, that is, P_N is approximated as

$$P_N=\frac{1}{V^N}\prod_{\substack{i,j=1\\ i<j}}^{N} g(\mathbf{r}_i-\mathbf{r}_j). \tag{62}$$

This approximation becomes exact on the pair level and describes the essential features of higher-order interactions in an approximate way. This approximation implies that

$$\nabla_1\ln\{P_N\}=\sum_{j=2}^{N}\nabla_1\ln g(\mathbf{r}_1-\mathbf{r}_j).$$

Substitution of this expression together with Eq. (48) into Eq. (58) for $N_C^{\mathrm{Br}}(t)$ readily leads to

$$\begin{aligned}N_C^{\mathrm{Br}}(t)=&\frac{\overline{\rho^2}}{\dot\gamma_s}k_BT\int d\mathbf{R}[\mathbf{C}(\mathbf{R}):\hat{\mathbf{\Gamma}}_s]\cdot\nabla_R g(\mathbf{R})\\&+\frac{\overline{\rho^3}}{\dot\gamma_s}k_BT\int d\mathbf{R}\int d\mathbf{r}g(\mathbf{R})g(\mathbf{r}-\mathbf{R})\\&\times\nabla_r g(\mathbf{r})\cdot[\mathbf{C}(\mathbf{R}):\hat{\mathbf{\Gamma}}_s].\end{aligned} \tag{63}$$

The first term on the right-hand side cancels against a term in $N_C^{\Phi}(t)$ in Eq. (60). The second term may be evaluated by decomposing each of the pair-correlation functions in its short- and long-range parts as in Eq. (59). The integrand in the second integral in Eq. (63) is thus written as

$$\begin{aligned}&\{1+h_l(\mathbf{R})+h_s(\mathbf{R})\}\{1+h_l(\mathbf{r}-\mathbf{R})+h_s(\mathbf{r}-\mathbf{R})\}\\&\quad\times\{\nabla_r h_l(\mathbf{r})+\nabla_r h_s(\mathbf{r})\}.\end{aligned}$$

Products of the short-range parts give rise to a regular contribution to the viscosity and may be disregarded. Furthermore, odd functions of $\mathbf{r}$ may be disregarded since these yield a zero result upon integration. Linearization of the above product with respect to the long-range parts then leaves the following terms to be analyzed:

$$\begin{gathered}h_l(\mathbf{r}-\mathbf{R})\nabla_r\mathbf{h}_s(\mathbf{r}),\quad h_l(\mathbf{r}-\mathbf{R})h_s(\mathbf{R})\nabla_r h_s(\mathbf{r}),\\h_l(\mathbf{R})h_s(\mathbf{r}-\mathbf{R})\nabla_r\mathbf{h}_s(\mathbf{r}),\quad h_s(\mathbf{r}-\mathbf{R})\nabla_r h_l(\mathbf{r}),\\h_s(\mathbf{R})h_s(\mathbf{r}-\mathbf{R})\nabla_r h_l(\mathbf{r}).\end{gathered}$$

In the first term $h_l(\mathbf{r}-\mathbf{R})$ may be Taylor expanded around $\mathbf{r}=\mathbf{0}$ since $h_s(\mathbf{r})$ is short ranged. Noting that $\mathbf{C}(\mathbf{R})$ is an odd function of $\mathbf{R}$, this term yields the following contribution to the viscosity:

The first term is

$$\begin{aligned}&-k_BT\frac{\overline{\rho^3}}{\dot\gamma_s}\int d\mathbf{r}\,\mathbf{r}\nabla_r h_s(\mathbf{r}):\\&\times\int d\mathbf{R}[\mathbf{C}(\mathbf{R}):\hat{\mathbf{\Gamma}}_s]\cdot\nabla_R h_l(\mathbf{R}).\end{aligned}$$

The second, third, and last terms are nonzero only when both $|\mathbf{r}|$ and $|\mathbf{R}|$ are less than or at most a few times R_V and therefore contribute only to the background viscosity. In the fourth term $h_l(\mathbf{r})$ may be Taylor expanded around $\mathbf{r}=\mathbf{R}$ to first order in gradients. Finally, $h_s(\mathbf{r})$ may be replaced by the equilibrium short-range part $h_s^{\mathrm{eq}}(r)$ of the total-correlation function since by definition this function is short ranged. This leads to the following contribution to the viscosity:

The fourth term is

$$\begin{aligned}&k_BT\frac{\overline{\rho^3}}{\dot\gamma_s}\int d\mathbf{r}\int d\mathbf{R}h_s(\mathbf{r}-\mathbf{R})\\&\quad\times[\mathbf{C}(\mathbf{R}):\hat{\mathbf{\Gamma}}_s]\cdot\nabla_R h_l(\mathbf{R})\\&=k_BT\frac{\overline{\rho^3}}{\dot\gamma_s}\int d\mathbf{r}'h_s(\mathbf{r}')\\&\quad\times\int d\mathbf{R}[\mathbf{C}(\mathbf{R}):\hat{\mathbf{\Gamma}}_s]\cdot\nabla_R h_l(\mathbf{R}).\end{aligned}$$

Putting things together, we arrive at the following expression for the anomalous contribution $N_C^{\mathrm{Br}}(t)$ to the shear viscosity:

$$N_C^{\mathrm{Br}}(t)=k_BT\frac{\overline{\rho^2}}{\dot\gamma_s}[1-C_s]\int d\mathbf{R}[\mathbf{C}(\mathbf{R}):\hat{\mathbf{\Gamma}}_s]\cdot\nabla_R h_l(\mathbf{R}), \tag{64}$$

where

$$C_s=-4\pi\overline{\rho}\int_0^{\infty}drr^2\left[h_s^{\mathrm{eq}}(r)-\frac{1}{3}r\frac{dh_s^{\mathrm{eq}}(r)}{dr}\right]. \tag{65}$$

This expression for C_s is accurate up to linear order in the bare Péclet numbers Pe^0 and Pe_s^0. Being related to the short-range part of the total correlation function, C_s is a well-behaved function at the critical point.

(iv) The contribution $N_r^{Br}(t)$. For identical colloidal particles, Eq. (58) for $N_r^{\mathrm{Br}}(t)$ is easily reduced to

$$N_r^{\mathrm{Br}}(t)=\frac{1}{2}\frac{\overline{\rho^2}}{\dot\gamma_s}k_BT\int_{R>d}d\mathbf{R}(\hat{\mathbf{\Gamma}}_s\cdot\mathbf{R})\cdot\nabla_R h_l(\mathbf{R}).$$

Here it is noted that only the long-range contribution h_l to the total-correlation function is relevant. An application of Gauss's integral theorem leads to a surface integral over the spherical surface with a radius d, the hard-core diameter of the colloidal particles, since $\nabla_R \cdot (\hat{\mathbf{\Gamma}}_s \cdot \mathbf{R}) = 0$. This integral probes the distortion of the total-correlation function at distances equal to d and therefore contributes only to the background viscosity.

There are two terms that possibly lead to anomalous behavior: the terms in Eqs. (60) and (64). Summing these terms yields

$$N(t) = k_B T \frac{\overline{\rho}^2}{\dot{\gamma}_s} \left[\beta \frac{d\Pi}{d\overline{\rho}} - C_s \right] \int d\mathbf{R} [\mathbf{C}(\mathbf{R}) : \hat{\mathbf{\Gamma}}] \cdot \nabla_R h_l(\mathbf{R}).$$

Since $\beta d\Pi / d\overline{\rho} \to 0$ on approach of the critical point, while C_s remains finite, the term $\sim \beta d\Pi / d\overline{\rho}$ may be neglected. The relevant expression for $N(t)$ that includes all the anomalous behavior is therefore

$$N(t) = k_B T \frac{\overline{\rho}^2}{\dot{\gamma}_s} C_s \int_{R>d} d\mathbf{R} [\mathbf{h}(\mathbf{R}) - h^{\mathrm{stat}}(\mathbf{R})] \nabla_R \cdot [\mathbf{C}(\mathbf{R}) : \hat{\mathbf{\Gamma}}_s], \tag{66}$$

where the index l on the total-correlation functions is omitted. Here Gauss's integral theorem is applied (the surface integral at $|\mathbf{R}| = d$ is omitted since it contributes only to the background viscosity) and

$$\int_{R>d} d\mathbf{R} h^{\mathrm{stat}}(\mathbf{R}) \nabla_R \cdot [\mathbf{C}(\mathbf{R}) : \hat{\mathbf{\Gamma}}_s] = 0.$$

is used. This follows from the fact that $h^{\mathrm{stat}}(x,y,z) = h^{\mathrm{stat}}(x,y,-z)$ and $\nabla \cdot [\mathbf{C}(\mathbf{R}) : \hat{\mathbf{\Gamma}}_s] \sim yz$ [see Eq. (49)], so that the integrand is an odd function of z. From the defining equation (15) of the structure factor it follows that the Fourier transform of $h(\mathbf{R}) - h^{\mathrm{stat}}(\mathbf{R})$ is equal to $[S(\mathbf{k},t) - S^{\mathrm{stat}}(\mathbf{k})]/\overline{\rho}$. Explicit expressions for $S(\mathbf{k})$ and $S^{\mathrm{stat}}(\mathbf{k},t)$ are given in Eqs. (29) and (33), respectively. We therefore rewrite Eq. (66) with the help of Parseval's theorem as

$$N(t) = \frac{1}{8\pi^3} k_B T \frac{\overline{\rho}}{\dot{\gamma}_s} C_s \int d\mathbf{k} \{S(\mathbf{k},t) - S^{\mathrm{stat}}(\mathbf{k})\} I(\mathbf{k}), \tag{67}$$

with [using Eq. (49)]

$$I(\mathbf{k}) = \int_{R>d} d\mathbf{R} \{\nabla_R \cdot [\mathbf{C}(\mathbf{R}) : \hat{\mathbf{\Gamma}}_s]\} \exp\{-i\mathbf{k} \cdot \mathbf{R}\}$$

$$= -\frac{5\pi}{4} a^3 \frac{\mathbf{k} \cdot \hat{\mathbf{\Gamma}}_s \cdot \mathbf{k}}{k^2} (kd)^2 f(kd), \tag{68}$$

where the cutoff function f is equal to

$$f(x) = [(5x^5 - 10x^3 - 120x)\cos x + (5x^4 - 30x^2 + 120)\sin x]/16x^5 - \frac{5}{16} x \int_x^\infty dz \frac{\sin z}{z}. \tag{69}$$

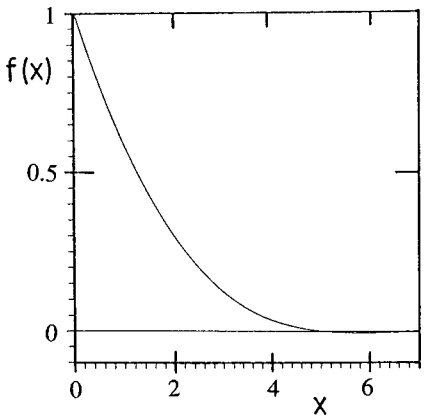

FIG. 6. Cutoff function $f(x)$ in Eq. (69).

The cutoff function is unity for $x = 0$: $f(0) = 1$. That the integral $I(\mathbf{k})$ is indeed equal to the expressions (68) and (69) is shown in Appendix C. The function f is called a cutoff function because it limits the integration range in the integral in Eq. (67) for $N(t)$ to small wave vectors. As can be seen from Fig. 6, where f is plotted, the cutoff function effectively limits the integration range to wave vectors $kd < 4$, while the major contribution is from wave vectors $kd < 2$. This is indeed the wavevector range for which the expression for the shear flow distorted structure factor as derived in Sec. III is valid. If the cutoff function would have had a longer range, extending to wave vectors for which $kd > 6$, corresponding to wavelengths of the order $d \approx R_V$ and smaller, we would have been forced to introduce in an *ad hoc* manner a finite upper limit for the wave-vector integration range in Eq. (67). Fortunately the introduction of such an uncontrolable cutoff wave vector is not necessary.

The final expressions for the viscoelastic response functions follow from substitution of the result (67) into Eq. (53),

$$\begin{Bmatrix} \eta_n'(\omega) \\ \eta_n''(\omega) \end{Bmatrix} = \frac{\omega C_s \overline{\rho} k_B T}{8\pi^4 \dot{\gamma}_s} \int_0^{2\pi/\omega} dt \begin{Bmatrix} \cos\{n\omega t\} \\ \sin\{n\omega t\} \end{Bmatrix} \int d\mathbf{k} \{S(\mathbf{k},t) - S^{\mathrm{stat}}(\mathbf{k})\} I(\mathbf{k}). \tag{70}$$

This expression will be rewritten in a dimensionless form in the next subsection.

A. Scaling forms for the viscoelastic response functions

The amplitude of $S(\mathbf{k},t) - S^{\mathrm{stat}}(\mathbf{k})$ is proportional to ξ^2. This follows from the linear relationship between S^{stat} and S^{eq} [see Eq. (29)] and that of S in Eq. (33) with S^{stat} and S^{eq}, while S^{eq} is proportional to ξ^2, according to Eq. (22). This can be made explicit by introducing the ''relative distortion''

$$\Psi_s(\mathbf{k},t) = \frac{S(\mathbf{k},t) - S^{\mathrm{stat}}(\mathbf{k})}{S^{\mathrm{eq}}(k)}. \tag{71}$$

This function is at most of order 1 in the entire (mean-field) vicinity of the critical point. An appropriate scaling relation for the response functions can be obtained from Eq. (70) by transforming the $\mathbf{k}$ integration to a $\mathbf{K} = \mathbf{k}\xi$ integration, by introducing the dimensionless shear rates λ and λ_s [Eq. (26)]

and the dimensionless time τ and frequency Ω [Eqs. (24) and (27)]. The viscoleastic response functions (70) are now written as

$$\begin{Bmatrix} \eta_n'(\omega)/\eta_0 \\ \eta_n''(\omega)/\eta_0 \end{Bmatrix} = C \begin{Bmatrix} N_n'(\lambda,\lambda_s,\Omega,\xi^{-1}d) \\ N_n''(\lambda,\lambda_s,\Omega,\xi^{-1}d) \end{Bmatrix}, \tag{72}$$

where η_0 is the shear viscosity of the solvent,

$$C = \frac{45}{256\pi^2}\varphi\left(\frac{d}{R_V}\right)^4 (\beta\Sigma/R_V^2)^{-2} C_s \tag{73}$$

is a constant, independent of shear rates, frequency, and correlation length, and $\varphi = (4\pi/3)a^3\overline{\rho}$ is the volume fraction of colloidal particles. The viscoelastic response scaling functions N_n' and N_n'' are thus simply proportional to the viscoelastic response functions $\eta_n'(\omega)$ and $\eta_n''(\omega)$, respectively. The microscopic expressions for these viscoelastic response scaling functions follow from Eqs. (70) and (71),

$$\begin{Bmatrix} N_n'(\lambda,\lambda_s,\Omega,\xi^{-1}d) \\ N_n''(\lambda,\lambda_s,\Omega,\xi^{-1}d) \end{Bmatrix} = \frac{-\Omega}{\lambda_s(\xi^{-1}d)\pi} \int_0^{2\pi/\Omega} d\tau \begin{Bmatrix} \cos\{n\Omega\tau\} \\ \sin\{n\Omega\tau\} \end{Bmatrix} \times \int d\mathbf{K} K_2 K_3 \frac{\Psi_s(\mathbf{K},\tau|\lambda,\lambda_s,\Omega)}{1+K^2} \mathbf{f}(K\xi^{-1}d), \tag{74}$$

where the relative distortion Ψ_s is now expressed in terms of dimensionless quantities and its shear rate and frequency dependence are denoted explicitly.

Explicit expressions for the relative structure factor distortion Ψ_s follow from Eq. (33) in the most general case of a superimposed oscillatory shear flow. Numerical results for the viscoleastic response functions in Eq. (74) must be obtained by numerical integration.

From the experimental point of view it is more convenient to express data as functions of a bare Péclet number $\sim\dot{\gamma}_s$ instead of the dressed Péclet number λ_s since the latter depends also on the distance from the critical point. A most convenient bare Péclet number is perhaps the following ''alternative bare Péclet number''

$$\mathrm{Pe}_s^\star \equiv \lambda_s(\xi^{-1}d)^4 = \frac{1}{\beta\Sigma/R_V^2}\left(\frac{d}{R_V}\right)^4 \mathrm{Pe}_s^0. \tag{75}$$

On the one hand, this bare Péclet number is equal to a product of two of the dimensionless numbers λ_s and $(\xi^{-1}d)^4$, which are relevant quantaties in the theory, while on the other hand it is directly proportional to the experimentally easily accessible bare Péclet number Pe_s^0 with a proportionality constant that is independent of the distance to the critical point.

It should be noted that the expression (74) represents only the anomalous parts of the response functions. The experimentally measured response functions are the sum of this anomalous contribution and a background contribution. Before comparing experimental results to the above predictions, these background contributions should be subtracted.

VI. RESPONSE TO A PURE OSCILLATORY SHEAR FLOW

In the following subsections we first consider the linear viscoelastic response to a pure oscillatory shear flow (where $\dot{\gamma}=0$) and then discuss nonlinear response characteristics. Numerical results for the viscoelastic response scaling functions are accurate to within 2%, or 0.002 for values of these functions smaller than about 0.05.

A. Linear response to pure oscillatory shear flow ($\lambda=0$)

In the absence of the stationary component of the shear flow ($\dot{\gamma}=0$) the viscoelastic response functions can be found from Eq. (74), where the relative structure factor distortion now follows from Eq. (37). The integrations can be done analytically only in the linear response regime, where the relative structure factor distortion reduces to simple analytic functions that follow from Eq. (40). Substitution of Eq. (40) into Eq. (74) leads to

$$N_1'(\lambda=0,\lambda_s\to 0,\Omega,\xi^{-1}d) = \frac{8\pi}{15(\xi^{-1}d)}\int_0^\infty dK \frac{K^8 f(K\xi^{-1}d)}{(1+K^2)[\Omega^2+K^4(1+K^2)^2]}, \tag{76}$$

$$N_1''(\lambda=0,\lambda_s\to 0,\Omega,\xi^{-1}d) = \frac{8\pi\Omega}{15(\xi^{-1}d)}\int_0^\infty dK \frac{K^6 f(K\xi^{-1}d)}{(1+K^2)^2[\Omega^2+K^4(1+K^2)^2]}. \tag{77}$$

The limiting expressions for these response functions on approach of the critical point, where $\xi^{-1}d\to 0$, are obtained by simply setting the cutoff function equal to unity: For very small values of $\xi^{-1}d$ the integral has already converged for k values such that $K\xi^{-1}d$ is still small and hence $f(K\xi^{-1}d)\approx 1$. Hence

$$N_1'(\lambda=0,\lambda_s\to 0,\Omega,\xi^{-1}d\to 0) = \frac{8\pi}{15(\xi^{-1}d)}\int_0^\infty dK \frac{K^8}{(1+K^2)[\Omega^2+K^4(1+K^2)^2]}, \tag{78}$$

$$N_1''(\lambda=0,\lambda_s\to 0,\Omega,\xi^{-1}d\to 0) = \frac{8\pi\Omega}{15(\xi^{-1}d)}\int_0^\infty dK \frac{K^6}{(1+K^2)^2[\Omega^2+K^4(1+K^2)^2]}. \tag{79}$$

These results predict a divergence of the viscosities η' and η'' as strong as the correlation length

$$\eta'\,\eta''\sim\xi. \tag{80}$$

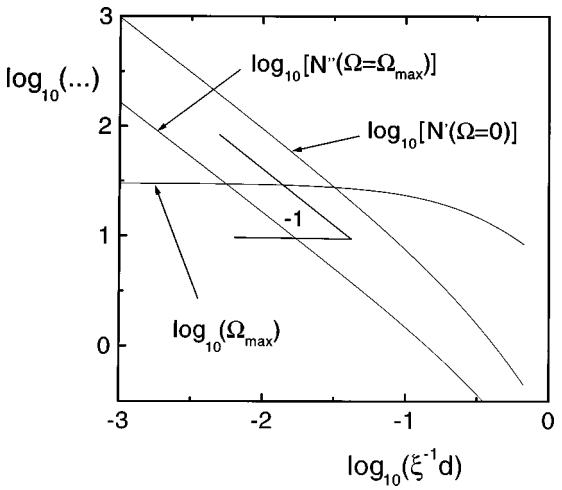

FIG. 7. Double logarithmic plots of the frequency $\Omega_{\max}$, where N'' exhibits its maximum, and of $N'(\Omega=0)$ and $N''(\Omega=\Omega_{\max})$ as functions of the inverse correlation length.

This behavior is illustrated in Fig. 7, where double logarithmic plots of $N'(\Omega=0)$ and $N''(\Omega=\Omega_{\max})$ as functions of the inverse correlation length are shown. Here $\Omega_{\max}$ is the dressed Deborah number where N'' exhibits its maximum. The scaling behavior in Eq. (80) is found to hold, on a double logarithmic scale, for $\xi/d>3$. The divergence of η' as predicted in Eq. (80) for a stationary shear flow ($\Omega=0$) was already predicted in Ref. [3] and experimentally verified for a colloid/polymer mixture in Ref. [4]. The critical exponent z_η in $\eta'(\dot{\gamma}_s\to 0,\omega=0)\sim\xi^{z_\eta}$ for molecular systems is known to be as small as 0.06 [1]. The much stronger divergence with $z_\eta=1$ of the steady shear, linear viscosity for colloidal systems is due to the long-range character of the fluid mediated interactions between the colloidal particles. The interactions of the colloidal particles through scattering of the incident flow field, quantified by the disturbance matrix in Eq. (47) and depicted in Fig. 5, indeed gives rise to the only surviving contribution to the anomalous part of the viscoelastic response functions in the mean-field region. Also shown in Fig. 7 is the frequency $\Omega_{\max}$ where N'' attains its maximum. As can be seen, $\Omega_{\max}$ is almost constant for $\xi/d>3$, again on a double logarithmic scale. From the defining equation (27) for Ω it follows that

$$\omega_{\max}\sim\xi^{-4}. \tag{81}$$

The frequency $\omega_{\max}$ at which η'' exhibits its maximum is thus predicted to shift to smaller values on approach of the critical point like ξ^{-4}.

For large frequencies the integrands in Eqs. (78) and (79) have poles $K^2\sim\sqrt{\Omega}$. It is easily seen from the residua theorem that both integrals now vary like $\sim\Omega^{-1/4}\sim\omega^{-1/4}$. An alternative derivation of this result, without the use of the residua theorem, is given in Appendix D. This high-frequency behavior is in contrast to the frequency dependence that has been found in case of hard-sphere-like suspensions without hydrodynamic interactions [26–29], where η' decays at high frequencies as $\sim\omega^{-1/2}$. Further away from the critical point, where Eqs. (76) and (77) are the proper expressions for the response functions, there is a faster decay with increasing frequency. This is most clearly seen in Figs.

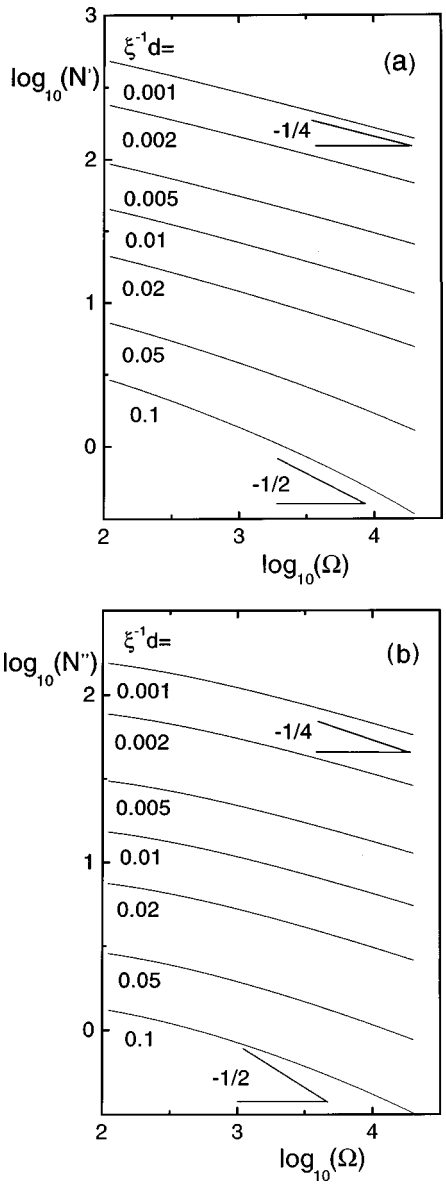

FIG. 8. Double logarithmic plots of (a) N' and (b) N'' as functions of the frequency Ω for various distances from the critical point (values of $\xi^{-1}d$ are indicated in the figures).

8(a) and 8(b) where double logarithmic plots of N' and N'' versus Ω are shown. The frequency dependence of N', away from the critical point, resembles an $\sim\Omega^{-1/2}$ kind of decay. There is thus a gradual cross-over from an $\sim\Omega^{-1/4}$ dependence close to the critical point to an $\sim\Omega^{-1/2}$ decay farther away from the critical point. In an experiment it will be difficult to achieve values of $\xi^{-1}d$ less than about 0.01, but it should still be possible to measure the approach toward the $\sim\omega^{-1/4}$ behavior. The reason for this kind of frequency dependence is as follows. Very close to the critical point the relaxation rates $\Gamma=D^{\text{eff}}k^2=D_0\beta[d\Pi/d\bar{\rho}+k^2\Sigma]k^2$ varies effectively like $\sim k^4$ since there $\beta d\Pi/d\bar{\rho}$ is a very small number. Further away from the critical point $\beta d\Pi/d\bar{\rho}$ becomes larger, so that relaxation rates Γ vary effectively like $\sim k^2$. Thus critical slowing down is responsible for the peculiar $\sim\omega^{-1/4}$ behavior very close to the critical point. Mathematically the crossover behavior can be seen from

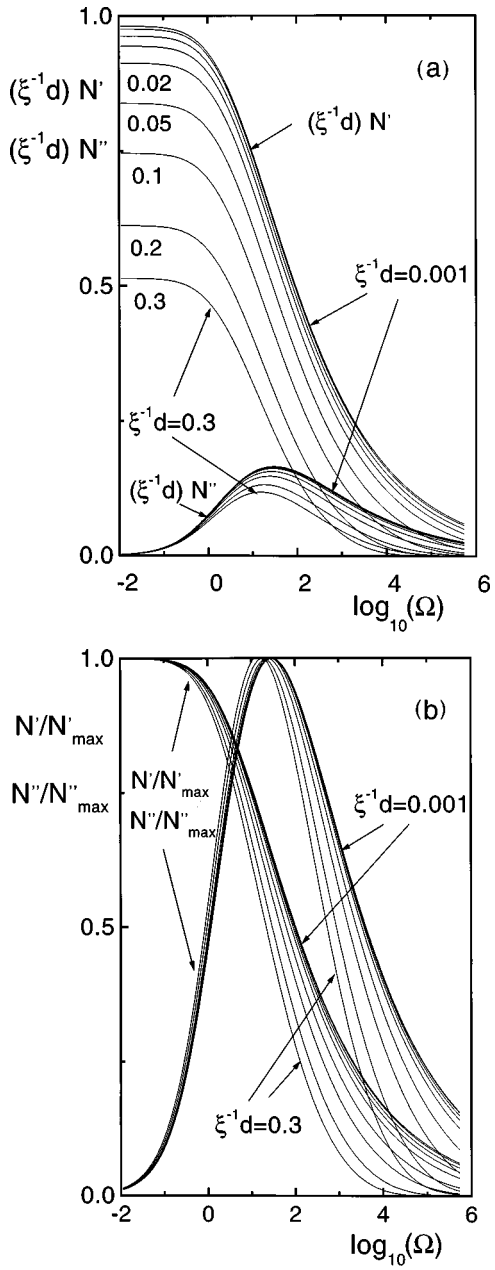

FIG. 9. (a) Plots of $(\xi^{-1}d)N'$ and $(\xi^{-1}d)N''$ versus the frequency (on a logarithmic scale) for various correlation lengths (from top to bottom $\xi^{-1}d=0.001$, 0.002, 0.005, 0.01, 0.02, 0.05, 0.1, 0.2, and 0.3). (b) Plots of N' and N'' versus the frequency (on a logarithmic scale) after normalization to their maximum values $N'(\Omega=0)$ and $N''(\Omega=\Omega_{\max})$, respectively, for the same correlation lengths as in (a).

Eqs. (76)–(79). In the expressions (78) and (79), which are valid close to the critical point, the major contribution to the integral stems from larger K values when Ω is large, so that in the denominator one may replace $1+K^2$ between the square brackets by K^2. This amounts to the neglect of $\beta d\Pi/d\overline{\rho}$ in the effective diffusion coefficient. Further away from the critical point, where Eqs. (76) and (77) are the appropriate expressions, the cutoff function limits the effective integration range to smaller K values, so that the same term $1+K^2$ becomes essentially equal to 1.

Figure 9(a) shows the frequency dependence of $(\xi^{-1}d)N'$ and $(\xi^{-1}d)N''$ for various correlation lengths. What is remarkable about the frequency dependence is that both η' and η'' are non-zero over a very large frequency range as compared to systems far away from the critical point. The frequency dependence becomes pronounced at $\Omega\approx 1$, as expected, but then the maximum for η'' occurs at relatively large frequencies. The reason for this broad frequency spectrum is as follows. Close to the critical point, $D^{\rm eff}(k=0)$ is small compared to the single-particle diffusion coefficient D_0 since $\beta d\Pi/d\overline{\rho}$ is small [see Eq. (16)]. A slight increase of the wave vector k then increases the diffusion coefficient $D^{\rm eff}(k)$ considerably, as indicated in Fig. 10. Further away from the critical point, where $\beta d\Pi/d\overline{\rho}$ is larger, the relative increase of the diffusion coefficient for finite wave vectors is less pronounced. Therefore, on approach of the critical point, a larger range of relaxation times comes into play and the frequency spectrum broadens. This is particularly clear from Fig. 9(b), where N' and N'' are normalized to their maximum values: The frequency spectrum for $\xi^{-1}d=0.001$ is seen to be a few decades broader than for $\xi^{-1}d=0.3$. For frequencies smaller than $\Omega_{\max}$, the response functions normalized to their maximum value are almost independent of the distance to the critical point.

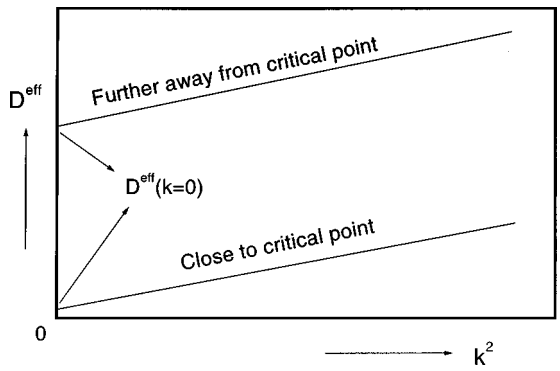

FIG. 10. Schematic illustration of the relative large increase $\sim k^2$ of the effective diffusion coefficient $D^{\rm eff}(k)$ at finite wave vectors very close to the critical point.

B. Nonlinear response to a pure oscillatory shear flow ($\lambda=0$)

On increasing the dimensionless shear rate λ_s beyond 1, the viscoelastic response to the oscillatory shearing motion becomes nonlinear. For a given correlation length $\xi^{-1}d=0.01$, viscoelastic response functions as obtained from Eqs. (37)–(39) and (74), where in Eq. (71) $S^{\rm stat}=S^{\rm eq}$ since $\dot\gamma=0$ are given in Fig. 11. It turns out that the even-indexed nonlinear response functions N''_{2n} and N'_{2n} with $n=1,2,\ldots$ are 0. Figure 11(a) shows that N'_1 decreases with increasing $\dot\gamma_s$ for low frequencies, but retains its linear response value at higher frequencies. The diminishing nonlinear effects on increasing the frequency was already mentioned in Sec. III E concerning the response of the structure factor. Notice in Fig. 11(a) the large plateau value of N'_1 as a function of the frequency, almost right up to the frequency where nonlinear effects disappear. The nonlinear viscoelastic response function N'_3 is plotted in Fig. 11(b). This response function is nonzero only for frequencies where the response function N'_1 differs from its linear response value. Figure 11(c) shows a

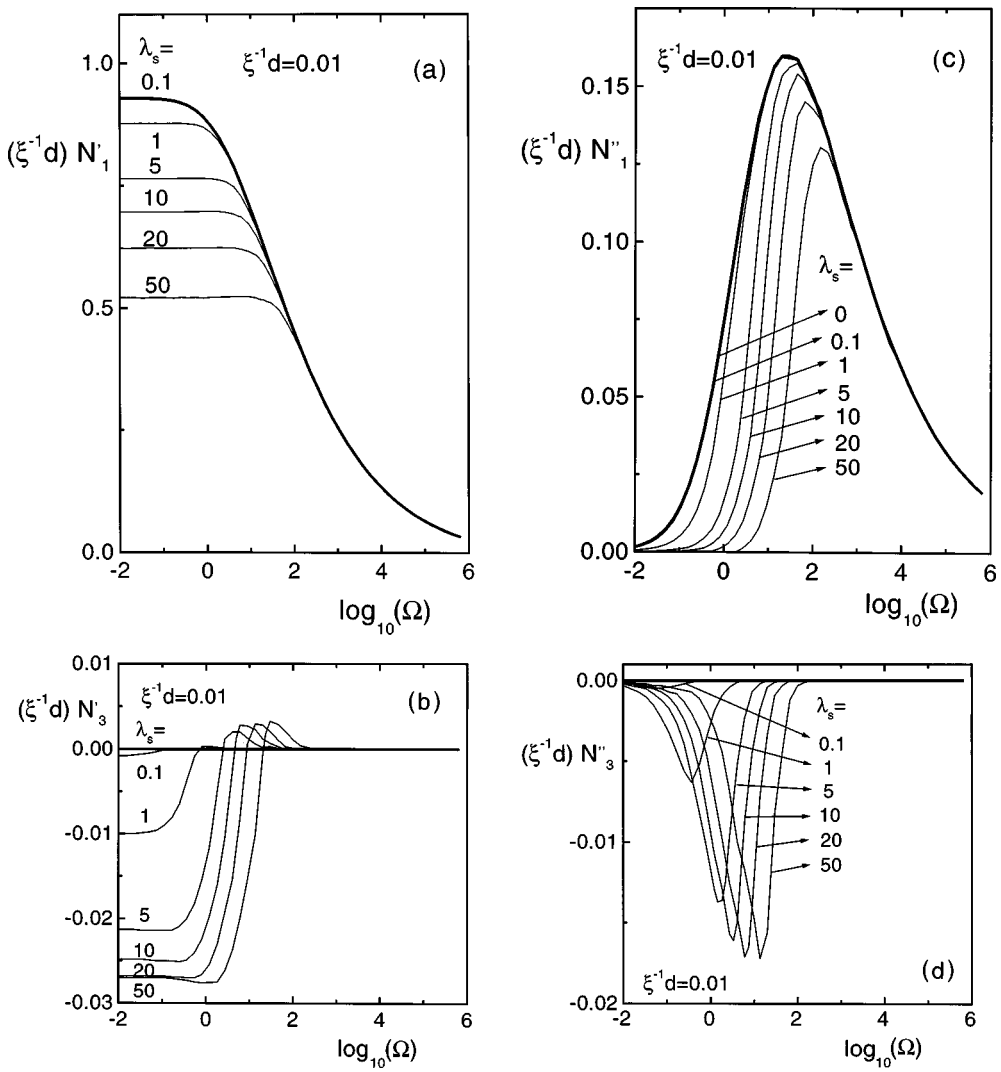

FIG. 11. Viscoelastic response functions as a function of the frequency for a given value $\xi^{-1}d=0.01$ of the correlation length: (a) N_1', (b) N_3', (c) N_1'', and (d) N_3''. In each figure the thick solid curve corresponds to linear response where $\lambda_s \to 0$. The values of λ_s are indicated in the figures.

similar behavior for the elastic response function N_1''. There is a decrease of this function with increasing shear rate $\dot{\gamma}_s$ up to a certain frequency beyond which the linear response values are retained. The frequency range beyond which N_1' retains its linear response values is smaller than the corresponding frequency range for N_1''. The nonlinear elastic response function N_3'' is plotted in Fig. 11(d). Notice that the effect of increasing λ_s beyond about 10 is a shift of the higher-order response functions N_3' and N_3'' to higher frequencies rather than an increase of their amplitude, contrary to the lowest-order functions N_1' and N_1'' which are not shifted but are only changed in amplitude.

Notice that since the bare Péclet number Pe_s^0 is a small number, the background viscoelastic response functions are in their linear response regime, despite the strong nonlinear response of the anomalous contribution of the response functions. The background contribution is related to stresses generated by the distortion of short-range correlations, while the anomalous contribution is due to the distortion of long-range correlations. Therefore, the background contribution to the nonlinear response functions is absent and experimental nonlinear response functions can be compared directly to theoretical predictions, without having to subtract a background contribution.

VII. ORTHOGONALLY SUPERIMPOSED OSCILLATORY SHEAR FLOW

In order to study the dynamic response of a stationary sheared microstructure by applying a superimposed oscillatory shear flow, the perturbing effect of the latter should be small. We therefore consider the *linear* viscoelastic response of a stationary sheared suspension to a superimposed oscillatory shear flow. The dressed Péclet number λ_s corresponding to the oscillatory flow is thus small, but the Péclet number λ corresponding to the stationary flow can be large. As in the preceding section, numerical results for the viscoelastic reponse scaling functions are accurate to within about 2%, or 0.002 for values of these functions smaller than about 0.05.

The viscoelastic response functions N' and N'' can be calculated from Eq. (74), where the relative structure factor distortion in Eq. (71) follows from Eqs. (33)–(35), with λ_s

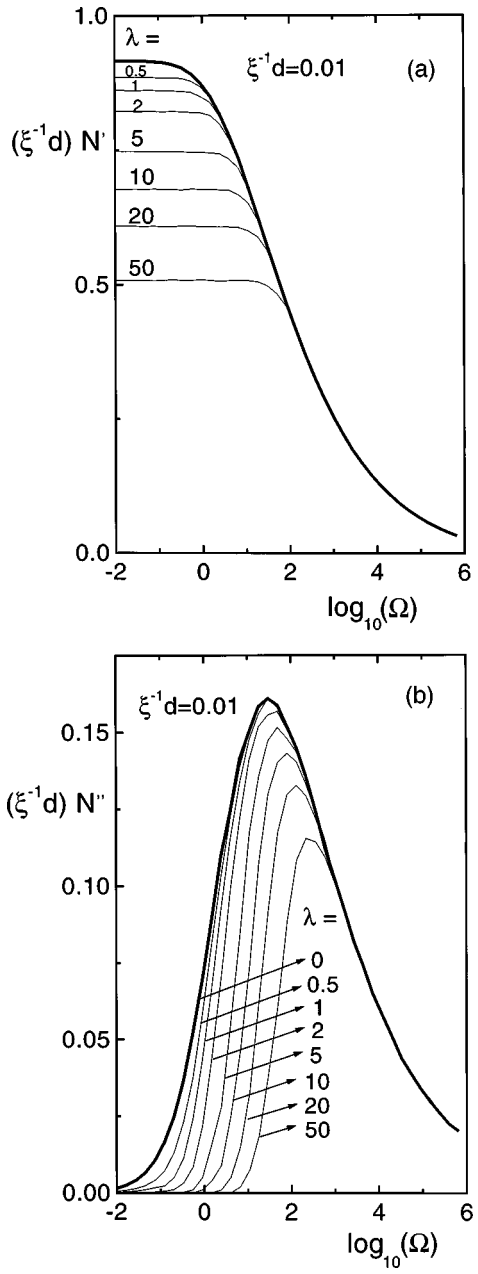

FIG. 12. Linear viscoelastic response functions for a given value $\xi^{-1}d=0.01$ of the correlation length of a stationary sheared system for dressed Péclet numbers λ as indicated in the figure: (a) N' and (b) N''. The thick solid line corresponds to $\lambda=<0$.

set equal to 0 in Eqs. (34) and (35). Keeping the λ_s dependence in Eqs. (34) and (35) corresponds to the more general case where the stationary sheared microstructure is affected by the oscillatory flow in a nonlinear fashion.

Numerical results for the linear response functions for a correlation length $\xi^{-1}d=0.01$ and for several values of λ are given in Fig. 12. There is a striking resemblance of these curves and the curves shown in Figs. 11(a) and 11(c), where the response functions of an otherwise quiescent suspension ($\lambda=0$) are plotted for values of λ_s where the response is highly nonlinear. Indeed we find the remarkable approximate relations

$$\eta'(\dot\gamma,\dot\gamma_s\to 0,\omega,\xi^{-1}d)\approx\eta_1'(\dot\gamma=0,\dot\gamma_s,\omega,\xi^{-1}d),$$

$$\eta''(\dot\gamma,\dot\gamma_s\to 0,\omega,\xi^{-1}d)\approx\eta_1''(\dot\gamma=0,\dot\gamma_s,\omega,\xi^{-1}d), \quad (82)$$

with $\dot\gamma=\dot\gamma_s$, where the first relation is found to be valid to within about 5% and the second to within about 10%. The linear viscoelastic response functions of a nonlinearly, stationary sheared system are thus approximately equal to the lowest-order response functions of an otherwise quiescent, nonlinear oscillatory sheared system.

VIII. SUMMARY AND CONCLUSIONS

The Smoluchowski equation allows a relatively straightforward derivation of the equation of motion for the long-range behavior of the pair-correlation function in the vicinity of the gas-liquid critical point. Fourier transformation yields an equation of motion for the structure factor [Eq. (25)], which contains three dimensionless parameters that characterize the flow field: two dressed Péclet numbers, pertaining to the stationary component λ [Eq. (26)] and the oscillatory component λ_s [Eq. (26)] of the shear flow, and a dressed Deborah number Ω [Eq. (27)]. This equation for $S(\mathbf{k},t)$ can be solved analytically [Eqs. (33)–(35)]. This expression reduces to simpler expressions for the case of pure stationary shear flow [Eqs. (29) and (30)] and in the case of pure oscillatory shear flow [Eqs. (37)–(39)]. Further simplification for a pure oscillatory shear flow in the case of linear response explicitly reveals the in-phase and out-of-phase component of the structure factor [Eq. (40)]: the out-of-phase component leads to an elastic component of the viscous response of the system. The nonlinear response of the microstructure occurs when the corresponding dressed Péclet numbers are larger than 1, while a significant frequency dependence is found when the dressed Deborah number is larger than 1. The dressed Péclet numbers vary like $\lambda\sim\dot\gamma\xi^{-4}$ and $\lambda_s\sim\dot\gamma_s\xi^{-4}$, where $\dot\gamma$ and $\dot\gamma_s$ are the shear rates for the stationary and oscillatory components of the flow, respectively. Similarly, the dressed Deborah number varies like $\Omega\sim\omega\xi^{-4}$, with ω the frequency of oscillation. In each case ξ is the correlation length of the quiescent, unsheared system. These scaling relations imply that on approach of the critical point a nonlinear response and frequency dependence will be found at decreasing shear rates and frequencies. In particular, the frequency where the elastic component $\eta''(\omega)$ exhibits its maximum in a linearly, pure oscillatory sheared system shifts to lower frequencies like $\sim\xi^{-4}$.

Microscopic expressions for (linear and nonlinear) viscoelastic response functions are equal to various Fourier components of a phase function [Eq. (53)] that can be evaluated explicitly in terms of a wave-vector integral [Eq. (74)] of the relative structure factor distortion [defined in Eq. (71)] and a cutoff function [Eq. (69)]. The cutoff function emerges naturally from the evaluation of the above-mentioned phase function as the Fourier transform of (the divergence of) the scattering contribution to the velocity of a colloidal particle [see Eq. (68)]. This cutoff function limits the wave-vector integration to wave vectors $k<4/d$, with d the core diameter of the spherical colloidal particles. The scattering contribution to the velocity of a colloidal particle is the additional

velocity that that colloidal partcile attains as a result of the solvent flow field generated by the cores of the remaining colloidal particles through scattering of the incident linear shear field. This solvent mediated interaction (referred to in colloid science as a ''hydrodynamic interaction'') is long ranged and leads to a much stronger divergence of viscoelastic response functions as compared to molecular systems, e.g., binary fluid mixtures. The critical exponent z_η for the zero-shear and zero-frequency viscosity η in $\eta \sim \xi^{z_\eta}$ is found to be equal to 1 in our mean-field treatment and should be contrasted with the very small value of 0.06 for molecular systems. Such a strong divergence is found both for the linear and the nonlinear viscoelastic response functions.

One may expect a gradual crossover of the critical exponent z_η from 1 to 0.06 when the dissolved particles become smaller and ultimately become equal in size to the solvent particles. The values 1 and 0.06 are the extreme values for z_η in the case of a colloidal system, where there is a clear separation in time scales for relaxation of microstructure of colloidal particles and of the solvent molecules, and in the case of binary fluid mixtures, where these relaxation times for both species are about equal. For polymer and protein solutions, for example, the exponent z_η is probably somewhere in between 1 and 0.06.

The lowest-order frequency-dependent viscoelastic response functions are found to attain their linear response values for larger frequencies. The nonlinear response thus disappears on increasing the frequency. At large frequencies the frequency dependence of the lowest-order response functions is found to vary like $\sim\omega^{-1/4}$ in the direct vicinity of the critical point and crosses over to a $\sim\omega^{-1/2}$ behavior further away from the critical point. The $\sim\omega^{-1/2}$ behavior is also found for hard-sphere-like colloids in the absence of hydrodynamic interactions, which do not exhibit a gas-liquid critical point. The crossover from a $\omega^{-1/2}$ to a $\omega^{-1/4}$ behavior on approach of the critical point is the result of critical slowing down. The relevant diffusion coefficient is $D^{\rm eff} = D_0\beta[d\Pi/d\bar{\rho} + k^2\Sigma]$, where D_0 is the single-particle diffusion coefficient, Π is the osmotic pressure, $\bar{\rho}$ is the number density of colloidal particles, and Σ is a constant that is well behaved at the critical point [see Eq. (16)]. Further away from the critical point and for the small wave vectors of interest, $D^{\rm eff} \approx D_0\beta(d\Pi/d\bar{\rho})$, while close to the critical point $D^{\rm eff} \approx D_0\beta k^2\Sigma$ since then $\beta d\Pi/d\bar{\rho}$ is a small number. This different wave-vector dependence of the diffusion coefficient away from the critical point and close to it is responsible for the different frequency dependence of the lowest-order viscoelastic response functions.

The explicit expressions derived in the present paper allow for the calculation of the entire frequency dependence of linear and nonlinear response functions (see Sec. VI for pure oscillatory flow and Sec. VII for superimposed shear flow). A surprising feature is that, to within about 10%, the linear viscoelastic response functions corresponding to an orthogonally superimposed oscillatory shear flow for systems subjected to a stationary shear flow are equal to the lowest-order response functions for a pure oscillatory shear flow, when $\dot{\gamma}$ for the former case is equal to $\dot{\gamma}_s$ in the latter case [see Eq. (82)].

The predicted strong divergence of the zero-shear and zero-frequency shear viscosity has been confirmed experimentally [4]. Experiments concerned with the frequency dependence and the nonlinear response have not been performed so far. Furthermore, the crossover behavior from $z_\eta = 1$ to $z_\eta = 0.06$ on decreasing the size of the dissolved species from the colloidal range to the molecular range has not been investigated experimentally.

ACKNOWLEDGMENTS

This work has benefited from discussions with Professor N. Wagner (University of Delaware) and Professor J. Mellema (University of Twente, The Netherlands).

APPENDIX A: SOLUTION OF EQ. (28)

In order to solve Eq. (28) we will need the following representation of the δ distribution: Let $f(X)$ denote a function in $\Re$, with $f'(X) \equiv df(X)/dX > 0$ and $\lim_{X\to\infty} f(X) = \infty$; then

$$\delta(X - X_0) = H(X - X_0) \lim_{\epsilon \downarrow 0} \frac{f'(X)}{\epsilon} \exp\left\{ - \frac{f(X) - f(X_0)}{\epsilon} \right\}, \tag{A1}$$

where $H(X) = 0$ for $X < 0$ and $H(X) = 1$ for $X \geqslant 0$, the Heaviside unit step function.

The differential equation (28) is solved by variation of constants. First consider the homogeneous equation, where $S^{\rm eq}$ is omitted,

$$\lambda K_1 \frac{\partial S^{\rm stat}(\mathbf{K})}{\partial K_2} = K^2[1 + K^2] S^{\rm stat}(\mathbf{K}).$$

Straightforward integration yields

$$S^{\rm stat}(\mathbf{K}) = C(K_1, K_3) \exp\left\{ \frac{1}{\lambda K_1} \int_0^{K_2} dY [K_1^2 + Y^2 + K_3^2] \times [1 + K_1^2 + Y^2 + K_3^2] \right\}.$$

Here C is an integration constant that is in general a function of K_1 and K_3 since we have integrated with respect to K_2. Substitution of the above expression into the differential equation, with C understood to be a function of K_2 as well, yields a differential equation for C, which is easily integrated to obtain

$$S^{\rm stat}(\mathbf{K}) = C' \exp\left\{ \frac{1}{\lambda K_1} \int_0^{K_2} dY [K_1^2 + Y^2 + K_3^2][1 + K_1^2 + Y^2 + K_3^2] \right\} - \frac{1}{\lambda K_1} \int^{K_2} dX [K_1^2 + X^2 + K_3^2] \times [1 + K_1^2 + X^2 + K_3^2] S^{\rm eq}(\sqrt{K_1^2 + X^2 + K_3^2}) \times \exp\left\{ \frac{1}{\lambda K_1} \int_X^{K_2} dY [K_1^2 + Y^2 + K_3^2] \times [1 + K_1^2 + Y^2 + K_3^2] \right\}.$$

This expression is finite for all $\mathbf{K}$'s when the integration constant C' is 0 and the unspecified lower integration limit

is $-\infty$ in case $\lambda K_1<0$ and $+\infty$ in case $\lambda K_1>0$. With $X_0=K_2$, $\epsilon=\lambda$, and $f(X)=(1/K_1)\int_0^X dY[K_1^2+Y^2+K_3^2][1+K_1^2+Y^2+K_3^2]$ in the representation (A1) for the δ distribution, the above expression (with $C'=0$) is easily seen to become equal to $S^{\rm eq}(K)$ for $\lambda\to 0$, as it should. Subtraction of $S^{\rm eq}(K)$ from both sides, using the δ distribution representation (A1), and substitution of the expression (22) for the equilibrium structure factor leads to Eqs. (29) and (30) for the static structure factor.

APPENDIX B: SOLUTION OF EQ. (32)

In order to solve the equation of motion (32), we write the structure factor as a function of K_1, the combination $K'=K_2+\lambda K_1\tau+(\lambda_s/\Omega)K_3\sin\{\Omega\tau\}$, K_3, and τ. In terms of the new coordinates $(\mathbf{K}',\tau)=(K_1,K',K_3,\tau)$ the equation of motion (32) reduces to,

$$\frac{\partial\Delta S(\mathbf{K}',\tau)}{\partial\tau}=-G^2[1+G^2]\Delta S(\mathbf{K}',\tau)+\frac{\lambda_s K_3}{\lambda K_1}G^2[1+G^2]\cos\{\Omega\tau\}\times\{S^{\rm stat}(K_1,K_2\to K'-F,K_3)-S^{\rm eq}(G)\},$$

where

$$F=\lambda K_1\tau+\frac{\lambda_s}{\Omega}K_3\sin\{\Omega\tau\}$$

and

$$G=\sqrt{K_1^2+(K'-F)^2+K_3^2}.$$

In the argument of the stationary structure factor, the string of symbols ''$K_2\to K'-F$'' means ''replace in the expression (29) K_2 by $K'-F$.'' This equation can be solved by variation of constants. The solution is found to be equal to

$$\Delta S(\mathbf{K}',\tau)=\frac{\lambda_s K_3}{\lambda K_1}\int_{-\infty}^{\tau}d\tau'\cos\{\Omega\tau\}G^2(\tau')[1+G^2(\tau')]\times\{S^{\rm stat}(K_1,K_2\to K'-F(\tau'),K_3)-S^{\rm eq}(G(\tau'))\}\exp\left\{-\int_{\tau'}^{\tau}d\tau''G^2(\tau'')\times[1+G^2(\tau'')]\right\}.$$

The initial conditions are eliminated by taking the lower integration limit in the outer integral equal to $-\infty$. The above expression is thus the limiting solution of the equation of motion after transients have died out. Returning to the original coordinates, and introducing the functions as defined in Eqs. (34) and (35) gives the representation in Eq. (33).

APPENDIX C: EVALUATION OF THE CUTOFF FUNCTION

In this appendix we evaluate the integral

$$I(\mathbf{k})=\int_{\mathbf{R}>d}d\mathbf{R}\{\nabla_R\cdot[\mathbf{C}(\mathbf{R}):\mathbf{\Gamma}]\}\exp\{-i\mathbf{k}\cdot\mathbf{R}\},$$

which appears in Eq. (67) for $N(t)$. Substitution of Eq. (49) for the divergence of the hydrodynamic function leads to

$$I(\mathbf{k})=\frac{75}{2}a^6\hat{\mathbf{\Gamma}}_s:\int_{\mathbf{R}>d}d\mathbf{R}\,R^{-4}\oint d\hat{\mathbf{R}}\hat{\mathbf{R}}\hat{\mathbf{R}}\hat{\mathbf{R}}\exp\{-i\mathbf{k}\cdot R\hat{\mathbf{R}}\},\tag{C1}$$

where the integral $\oint d\hat{\mathbf{R}}(\,)$ with respect to the spherical angular coordinates ranges over the entire unit spherical surface. This integral is equal to

$$\oint d\hat{\mathbf{R}}\hat{\mathbf{R}}\hat{\mathbf{R}}\hat{\mathbf{R}}\exp\{-i\mathbf{k}\cdot R\hat{\mathbf{R}}\}=-\frac{1}{R^2}\nabla_k\nabla_k\oint d\hat{\mathbf{R}}\exp\{-i\mathbf{k}\cdot R\hat{\mathbf{R}}\}=-\frac{4\pi}{R^2}\nabla_k\nabla_k\frac{\sin\{kR\}}{kR},$$

with ∇_k the gradient operator with respect to $\mathbf{k}$. Now using that $\nabla_k g(k)=\hat{\mathbf{k}}dg(k)/dk$, with $\hat{\mathbf{k}}=\mathbf{k}/\mathbf{k}$, for a differentiable function g of $k=|\mathbf{k}|$, yields

$$\nabla_k\nabla_k\frac{\sin\{kR\}}{kR}=\hat{\mathbf{I}}R^2\frac{1}{kR}\frac{d}{d(kR)}\frac{\sin\{kR\}}{kR}+\mathbf{kk}R^4\frac{1}{kR}\frac{d}{d(kR)}\times\left[\frac{1}{kR}\frac{d}{d(kR)}\frac{\sin\{kR\}}{kR}\right].$$

Substitution of this result into Eq. (C1) and using that $\hat{\mathbf{\Gamma}}_s:\hat{\mathbf{I}}=0$ yields Eq. (68)

$$I(\mathbf{k})=-\frac{5\pi}{4}a^3\frac{\mathbf{k}\cdot\hat{\mathbf{\Gamma}}_s\cdot\mathbf{k}}{k^2}(kd)^2f(kd),$$

where (with $z=kR$)

$$f(x)=15x\int_x^\infty dz\frac{1}{z^3}\frac{d}{dz}\left[\frac{1}{z}\frac{d}{dz}\frac{\sin\{z\}}{z}\right].$$

Two partial integrations gives

$$f(x)=15x\left[-\frac{\cos\{x\}}{x^5}-\frac{2\sin\{x\}}{x^6}+15\int_x^\infty dz\frac{\sin\{z\}}{z^7}\right].\tag{C2}$$

This function may seem to be divergent at $x=0$ at first sight. However, the sum of the divergent contributions from the three separate terms add up to 0. This is most easily seen by rewriting the integral by means of successive partial integrations

$$\int_x^\infty dz\,\frac{\sin\{z\}}{z^7} = -\frac{1}{6}\int_x^\infty dz\,\sin\{z\}\frac{d}{dz}z^{-6}$$

$$= \frac{1}{6}\,\frac{\sin\{x\}}{x^6} + \frac{1}{6}\int_x^\infty dz\frac{\cos\{z\}}{z^6}$$

$$= \frac{1}{6}\,\frac{\sin\{x\}}{x^6} - \frac{1}{30}\int_x^\infty dz\,\cos\{z\}\frac{d}{dz}z^{-5} = \cdots$$

$$= \sin\{x\}\left(\frac{1}{6x^6} - \frac{1}{120x^4} + \frac{1}{720x^2}\right) + \cos\{x\}$$

$$\times\left(\frac{1}{30x^5} - \frac{1}{365x^3} + \frac{1}{720x}\right)$$

$$- \frac{1}{720}\int_x^\infty dz\,\frac{\sin\{z\}}{z}.$$

Substitution of this expression for the integral into Eq. (C2) for the function f yields Eq. (69). The value of this function for $x=0$ may now be evaluated by Taylor expansion of the sine and cosine functions and is thus found to be equal to 1.

APPENDIX D: HIGH-FREQUENCY BEHAVIOR

The asymptotic high-frequency behavior of η' close to the critical point in the case of pure oscillatory shear flow can be found from Eq. (78) as follows. For $\Omega \gg 1$ the integral converges for $K \gg 1$, so that Eq. (78) can be approximated by

$$\eta' \sim \int_0^\infty dK \frac{K^6}{\Omega^2 + K^8}.$$

Introducing the integration variable $x = \Omega^{-1/4}K$ leads to

$$\eta' \sim \Omega^{-1/4}\int_0^\infty dx\,\frac{x^6}{1+x^8} \sim \Omega^{-1/4}.$$

The same analysis applies to η'' as given by Eq. (79). This asymptotic behavior for large frequencies also follows from the residua theorem as stated in the main text.

[1] J. C. Nieuwoudt and J. V. Sengers, J. Chem. Phys. **90**, 457 (1989). This is a reevaluation of the viscosity exponent for a number of experiments on binary fluids.

[2] P. C. Hohenberg and B. I. Halperin, Rev. Mod. Phys. **49**, 435 (1977). This is a review on earlier theories on dynamical critical phenomena.

[3] J. K. G. Dhont, J. Chem. Phys. **103**, 7072 (1995).

[4] I. Bodnár and J. K. G. Dhont, Phys. Rev. Lett. **77**, 5304 (1996).

[5] L. D. Landau and E. M. Lifshitz, *Fluid Mechanics* (Pergamon, Oxford, 1979), paragraph 24, p. 88.

[6] D. van den Ende, J. Mellema, and C. Blom, Rheol. Acta **31**, 194 (1992).

[7] J. Zeegers, D. van den Ende, C. Blom, E. G. Altema, G. J. Beukema, and J. Mellema, Rheol. Acta **34**, 606 (1995).

[8] A. Onuki, K. Yamazaki, and K. Kawasaki, Ann. Phys. (N.Y.) **131**, 217 (1981).

[9] A. Onuki, J. Phys.: Condens. Matter **9**, 6119 (1997).

[10] J. F. Schwarzl and S. Hess, Phys. Rev. A **33**, 4277 (1986).

[11] D. Ronis, Phys. Rev. A **29**, 1453 (1984).

[12] N. J. Wagner and W. B. Russel, Physica A **155**, 475 (1989).

[13] R. M. Mazo, J. Stat. Phys. **1**, 89 (1969); **1**, 101 (1969); **1**, 559 (1969).

[14] J. M. Deutch and I. J. Oppenheim, J. Chem. Phys. **54**, 3547 (1971).

[15] T. J. Murphy and J. L. Aguirre, J. Chem. Phys. **57**, 2098 (1972).

[16] J. K. G. Dhont, *An Introduction to Dynamics of Colloids* (Elsevier, Amsterdam, 1996), Chap. 4.

[17] M. Fixman, J. Chem. Phys. **33**, 1357 (1960).

[18] More precisely, these Péclet numbers are assumed to be smaller than $R_V|d\ln\{g\}/dr_{|_+}|$, with $d\ln\{g\}/dr_{|_+}$ the contact value of the slope of the logarithm of the pair-correlation function. This follows from a comparison of the magnitude of the term $\sim\nabla_r g$ between the curly brackets in Eq. (5) and $\mathbf{\Gamma}\cdot\mathbf{r}g$, the last term in Eq. (5). When the latter term is small in comparison to the former, shear-induced distortions are small. Since the slope at contact may be large for attractive particles, short-range distortions may be negligible even for larger values of the bare Péclet numbers.

[19] J. K. G. Dhont, Phys. Rev. Lett. **76**, 4269 (1996).

[20] M. Fixman, Adv. Chem. Phys. **6**, 175 (1964). This estimate is obtained as follows. Whenever $(R_V - d)/d \ll 1$ (with d the core diameter of the colloidal particles) we may approximate Eq. (13) as

$$\beta\Sigma/R_V^2 \approx \beta\frac{2\pi}{15}\bar{\rho}\int_0^\infty dr' r'^3 \frac{dV(r')}{dr'}\left\{g^{\rm eq}(r') + \frac{1}{8}\bar{\rho}\frac{dg^{\rm eq}(r')}{d\bar{\rho}}\right\}$$

since the integration effectively ranges from d to R_V. Close to the critical point $\beta d\Pi/d\bar{\rho}$ is small, so that, from Eq. (12),

$$\frac{d}{d\bar{\rho}}\left[\beta\frac{2\pi}{3}\bar{\rho}^2\int_0^\infty dr' r'^3\frac{dV(r')}{dr'}g^{\rm eq}(r')\right] \approx 1.$$

It follows that $\beta\Sigma/R_V^2 \approx 1/10$, which is to be regarded as an order of magnitude estimate.

[21] H. E. Stanley, *Introduction to Phase Transitions and Critical Phenomena* (Oxford University Press, New York, 1971), Chap. 7.

[22] G. K. Batchelor, J. Fluid Mech. **83**, 97 (1977).

[23] G. K. Batchelor, J. Fluid Mech. **56**, 375 (1972).

[24] The effect of the hydrodynamic interaction on the shear rate dependence of the total-correlation function makes the integral nonabsolutely convergent (see [22] and [25]). Since we neglected hydrodynamic interaction as far as the distortion of

the pair-correlation function is concerned, this problem does not occur here.
[25] N. J. Wagner and B. J. Russel, Physica A **155**, 475 (1989).
[26] B. Cichocki and B. U. Felderhof, Phys. Rev. A **43**, 5405 (1991).
[27] R. A. Lionberger and W. B. Russel, J. Rheol. **38**, 1885 (1994).
[28] R. Verberg, I. M. de Schepper, and E. G. D. Cohen, Phys. Rev. E **55**, 3143 (1997).
[29] R. Verberg, I. M. de Schepper, M. J. Feigenbaum, and E. G. D. Cohen, J. Stat. Phys. **87**, 1037 (1997).